AD_____

Award Number: DAMD17-99-1-9145

TITLE: Role of Nuclear Receptor Coregulators in Hormone Resistant Breast Cancer

PRINCIPAL INVESTIGATOR: Lisa Nitao, Ph.D
Kathryn B. Horowitz, Ph.D

CONTRACTING ORGANIZATION: University of Colorado Health Sciences Center
Denver, CO 80262

REPORT DATE: September 2003

TYPE OF REPORT: Annual Summary

PREPARED FOR: U.S. Army Medical Research and Materiel Command
Fort Detrick, Maryland 21702-5012

REPORT DOCUMENTATION PAGE

Form Approved
OMB No. 074-0188

1. AGENCY USE ONLY (Leave blank)	2. REPORT DATE	3. REPORT TYPE AND DATES COVERED
	September 2003	Annual Summary (1 Sep 1999 - 31 Aug 2003)

4. TITLE AND SUBTITLE
Role of Nuclear Receptor Coregulators in Hormone Resistant Breast Cancer

5. FUNDING NUMBERS
DAMD17-99-1-9145

6. AUTHOR(S)
Lisa Nitao, Ph.D.
Kathryn B. Horowitz, Ph.D.

7. PERFORMING ORGANIZATION NAME(S) AND ADDRESS(ES)
University of Colorado Health Sciences Center
Denver, CO 80262

E-Mail: LISA.NITAO@UCHSC.EDU

8. PERFORMING ORGANIZATION REPORT NUMBER

9. SPONSORING / MONITORING AGENCY NAME(S) AND ADDRESS(ES)
U.S. Army Medical Research and Materiel Command
Fort Detrick, Maryland 21702-5012

10. SPONSORING / MONITORING AGENCY REPORT NUMBER

11. SUPPLEMENTARY NOTES
Original contains color plates: ALL DTIC reproductions will be in black and white

12a. DISTRIBUTION / AVAILABILITY STATEMENT
Approved for Public Release; Distribution Unlimited

12b. DISTRIBUTION CODE

13. ABSTRACT (Maximum 200 Words)

We propose that coregulatory proteins influence the direction of transcription by antagonist-occupied steroid receptors. We screened for such proteins and identified three cDNA fragments encoding peptides that interact with antagonist-bound PRs. The aims were to clone complete cDNAs; define the role of the unknown proteins on receptor activity; and determine the role of the unknown proteins in hormone dependency of breast cancers. Major findings: We have focused on one novel cDNA fragment, designated ORF#93. We cloned the full-length cDNA; localized the gene to chromosome 15q23.1; expressed the full-length protein; defined its tissue distribution; and determined that it is cytoplasmic. ORF#93 doesn't appear to have a ligand-specific effect on PR transcription, but it does have general transcriptional effects. From mammalian two-hybrid and GST pull-down assays, we've determined that ORF#93 interacts with hsp90 and that this is influenced by the presence of PR and its ligands. It's possible that ORF#93 functions to regulate key events in the formation of nascent PR, cytoplasmic chaperone interactions and translocation into the nucleus. If so, ORF#93 may play a key role in bringing PR to associate with cytoplasmic molecules with which PR would otherwise not interact.

14. SUBJECT TERMS
Breast cancer, tamoxifen, coregulators, steroid receptors

15. NUMBER OF PAGES
75

16. PRICE CODE

17. SECURITY CLASSIFICATION OF REPORT	18. SECURITY CLASSIFICATION OF THIS PAGE	19. SECURITY CLASSIFICATION OF ABSTRACT	20. LIMITATION OF ABSTRACT
Unclassified	Unclassified	Unclassified	Unlimited

Table of Contents

INTRODUCTION

Subject. The antiestrogen tamoxifen is one of the most effective hormonal agents for treatment of estrogen (ER) and progesterone (PR) receptor-positive breast cancers. However, development of resistance to tamoxifen is common, and is a major obstacle to long-term treatment success (Barker, 2003; Crawford et al., 1987; Horwitz, 1993). Tamoxifen, and the antiprogestin RU 486, are "mixed antagonists" having both agonist and antagonist properties (Gronemeyer et al., 1992). We have shown that the balance between agonist *vs.* antagonist transcriptional activities can be influenced by the abundance of nuclear receptor coregulatory proteins: the corepressors N-CoR and SMRT suppress the partial agonist activities of tamoxifen and RU486, while the coactivator L7/SPA enhances their partial agonist activity (Graham et al., 2000; Jackson et al., 1997).

Purpose. However, these coregulators are unlikely to be the sole players in transcriptional regulation by ER and PR under the influence of antagonists. We proposed that the full complement of coregulatory proteins that could influence the direction of transcription by antagonist-occupied steroid receptors had yet to be completely identified. L7/SPA is the only antagonist-specific coactivator defined to date. It is unlikely to be the only, or even the most important, protein to have this property. Similarly, it is unlikely that SMRT and N-CoR are the only corepressors that interact with antagonist-occupied steroid receptors. We believe that these three represent a minor subset of the whole, for two reasons. First, screening for coregulators has not focused on receptor N-termini, yet AF1 may be critical to the agonist effects of mixed antagonists. Newer experimental strategies may correct this deficiency. Second, recent crystallographic analyses show subtle structural variations in the conformation of the C-terminal ligand binding domain, dictated by the identity of the ligand. For the most part, protein interaction screens for C-terminal binding proteins have not used antagonists. **We proposed to use an antagonist-biased screen to identify true antagonist-specific coregulators.**

Scope. In preliminary studies, we identified three partial cDNA clones encoding proteins that specifically interacted with antagonist-bound PRs. We proposed to clone the complete cDNAs and define their structure (Aim 1); to define the role of the unknown proteins on receptor activity (Aim 2); and, if they look promising, to determine the role of these proteins in hormone dependency of breast cancers (Aim 3). In the first year we focused on one novel cDNA fragment, designated ORF#93, whose features highlighted it as particularly interesting and relevant to our hypothesis. Therefore, the research effort was focused on completely cloning and characterizing this gene and its protein product. The results obtained continued to suggest that this protein may play an important role in nuclear receptor function, and new approaches were taken to elaborate the role of the ORF#93 protein.

Task 1: To clone, sequence and define the structure of three novel, antagonist-specific, ER- and PR-interacting proteins

Clone and sequence full length ORF#93

5'RACE (rapid amplification of cDNA ends) was carried out using Clontech's SMART RACE technology. mRNA from HeLa cervicocarcinoma cells and T47D breast cancer cells, was reverse transcribed using an oligo (dT) primer. A universal primer was tethered to the 5'-end of the 1st strand cDNA by targeting the dCTP-rich tail added to the end of the newly synthesized strands by reverse transcriptase. This allowed 5'-targeted PCR amplification of the 1st strand cDNA using the universal forward primer and a gene-specific reverse primer. **Figure 1A** indicates the location of the primers used, with respect to the most 5' ORF#93 clone originally retrieved from screening a λgt11 HeLa cell cDNA library. This clone contained a 3.1kb ORF#93 cDNA but lacked the complete 5'-end of the gene. The following oligos were designed: two reverse primers, R1 and R2, that hybridized to the 5'-end of the cDNA; an oligonucleotide probe, S1, for Southern blotting the subsequent RACE products; two primers, F+ and R+, to hybridize with the 3'-end of the cDNA and act as an internal control for the presence of the template in the RACE product; and a λgt11 vector primer, gt11F, to use as a PCR control with the λgt11 ORF#93 phage as template.

PCR amplification of RACE cDNA using the RACE forward primer and either R1 (see appendix, **Figure 1B**, lanes 1 and 6) or R2 (**Figure 1B**, lanes 2 and 7) produced multiple faint bands on an ethidium bromide stained agarose gel. Using the same RACE cDNA template (lanes 3 and 8), the λgt11 clone (lanes 5 and 10) or a plasmid vector containing the 3.1kb ORF#93 insert, the internal primers F+ and R+ produced a band of the expected size (1003bp). Primers gt11F and R2 produced the expected 230bp fragment when the λgt11 clone was used as template (lanes 4 and 9). A no template control was completely negative with RACE forward primer and R2 (lane 11). The PCR products were Southern blotted, and probed using S1. As expected, the 230bp control fragment (**Figure 1C**, lanes 4 and 9) strongly hybridized to the probe, whereas the 1003bp fragment was not detected. Strong bands were detected at 200 to 300bp in the RACE products amplified using RACE forward primer and R1 (lanes 1 and 5) or R2 (lanes 2 and 6). Primer R2 produced a band that was slightly larger than the band produced by R1, and the difference appeared similar to the distance between the start of the two primers (52bp). The fragments were subcloned and several clones were sequenced. Additional 5'-sequence of ORF#93 was obtained, which a potential start codon 62bp upstream of the existing clone. Further sequencing upstream of this ATG revealed an in frame stop codon at –114bp, respective to the new start site, suggesting that the full gene had been cloned. Using a unique KasI site at the 5'-end of ORF#93, the sequence identified by 5'-RACE was combined with the rest of the cDNA to make a full-length 3.1kb clone. **These experiments generated the entire protein coding sequence.**

At the same time as RACE cloning of the full ORF#93 cDNA was achieved, the sequence of a 156089bp genomic clone containing an unorganized series of 9 contigs was made available on the high throughput genomic database (Accession code AC004886). **This information, together with the protein coding sequence, allowed us to determine the genomic structure of ORF#93**. The DNA is organized into 20 exons and is located on chromosome 15q26.1. The first intron (**Figure 2**) is 166bp and falls upstream of the 5'-end of the 3.1kb clone, and downstream of the first methionine and in-frame stop codon. This assignment was confirmed by primer-specific RT-PCR spanning the TGA and first ATG, since several

potential splice sites were contained in this region. **These experiments defined the transcription start-site for the longest ORF#93 transcript.**

Analyze the ligand dependency and specificity of interactions between the three proteins (ORF#61, ORF#93 and ORF#127), PR and ER using a mammalian two-hybrid system and GST pull-down assays and analyze the interactions of the three proteins with other members of the nuclear receptor family

The full-length ORF#93 cDNA was subcloned into pGEX 4T-1, downstream from the sequence encoding glutathione S-transferase (GST), and a GST-93 fusion protein was produced in E.coli. The purified protein was bound to glutathione sepharose and used in a series of GST pull-down experiments with PR-A or -B, glucocorticoid receptors (GR) or ER, all over-expressed in HeLa cells. GST-93 interacted with PR-A, PR-B, and GR, whether unliganded or in the presence of agonist or antagonist (**Figure 3**). The strongest binding observed was with unliganded or antagonist-bound receptors. Little or no binding was observed to GST alone, suggesting that the interaction was specific for GST-93. GST-93 also bound to ERs, and the specificity of this interaction is still being confirmed. Thus, the **ORF# 93 protein appears to interact with PR and GR either in the unliganded, or antagonist-occupied state.**

Additional studies on the binding of this protein to PR were done in collaboration with the laboratory of David O. Toft at the Mayo Clinic (Rochester, MN). To facilitate the studies, a monoclonal antibody to ORF#93 was made using bacterially expressed and purified protein. This antibody (AbS1) is effective both for western blotting and for immunoprecipitation studies. Immunoprecipitation was used to further study the binding of endogenous ORF#93 to both progesterone receptor forms A and B. Two variants of the human breast cancer cell line T47D were analyzed; one, YA, expressing exclusively the PR-A isoform and the other, YB, expressing exclusively PR-B. Antibodies were used to specifically immunoprecipitate PR-A, PR-B, or ORF#93 from cell lysates and the immunoprecipitated proteins were resolved by SDS-PAGE and analyzed by western blotting. As shown in **Figure 4A**, ORF#93 was detected in complexes with each PR species. When an antibody to ORF#93 (AbS1) was used for immunoprecipitation, co-precipitation of PR-A was clearly observed, but that for PR-B was barely detectable with this technique. Thus, both receptor species can be observed in complexes with ORF#93, although their abundance in these complexes may differ.

The PR in cytosolic extracts is known to exist in complex with hsp90. Therefore, an antibody to hsp90 (H9010) was used to test for the co-precipitation of ORF#93 with hsp90 (**Figure 4B**). A Western blot using an antibody for ORF#93 clearly indicated its presence in complex with hsp90. Taken together, these results further expanded the protein multicomplexes of PR-A, PR-B and hsp90 to contain ORF#93.

Define the tissue distribution for the three receptor interacting proteins using human tissue RNA blots; their developmental expression using fetal mouse blots; and prepare polyclonal antibodies for subcellular localization studies.

The 3.1kb ORF#93 cDNA was labelled by ^{32}P-dCTP random priming, and used to probe a Clontech multi-tissue RNA master blot. The blot contained equal amounts of dot blotted RNA from 43 adult human tissues, seven fetal tissues, and eight controls which included yeast, E.coli and human RNA and DNA. Trace amounts of ORF#93 transcript were detected in most tissues (**Figure 5**) suggesting that as with other coregulatory proteins, ORF#93 is ubiquitously expressed at limiting levels. **The strongest expression of the gene was seen in lung and**

kidney. Expression was also clearly detectable in a number of potential nuclear receptor targets, such as ovary, testis, adrenal, pituitary and mammary gland. Interestingly, expression was much lower in fetal lung and kidney than in the adult, suggesting that ORF#93 plays a more important role in the adult. No hybridization of the probe was observed to the negative controls, except to E.coli and human DNA. Hybridization to E.coli DNA but not yeast DNA or yeast or E.coli RNA simply suggests some degree of homology to bacterial sequences. Hybridization to the human DNA control suggests three possibilities: the gene is highly expressed, or it contains repetitive sequence, or it is a member of a multi-gene family. The last of these three is most likely since the transcript is not very abundant, and no hybridization of the probe was seen to the other repetitive sequence control (C_0t-1 DNA). This may be due to the **presence of three tetratricopeptide (TPR) repeat domains in the coding sequence of ORF#93**. The TPR motif is a degenerate 34 amino acid sequence that is found on several co-chaperones, in particular those that interact with hsp90 (Barent et al., 1998; Young et al., 1998). It is often found in multiple copies and in tandem arrays (Blatch and Lassle, 1999; Lamb et al., 1995). As will be discussed later, the TPR motifs appear to play an important role in the interaction of ORF#93 with other proteins. Therefore, while informative, these results suggest that it may be important to confirm this finding using a truncated cDNA probe lacking these TPR sequences.

A polyclonal antibody to ORF#93 was produced using a peptide sequence predicted to be antigenic from the total protein sequence. **The antibody detects recombinant, denatured ORF#93 on immunoblots.** The protein has an apparent molecular weight of 103 kDa (**Figure 6**). The polyclonal does not recognize the folded native protein. Additionally, we have been unable to detect the endogenous protein in HeLa or T47D cells using this antibody, even under denaturing conditions, suggesting that **ORF#93 is present in limiting quantities in these cells.**

Perform RT-PCR using ORF#127 specific primers to clone and sequence full length ORF#127 cDNA

This remains to be completed, as we have chosen to focus on ORF#93.

Task 2: To define the transcriptional coregulatory or other functional properties of the receptor-interacting proteins

Clone the three receptor interacting proteins into expression vectors

The full-length ORF#93 cDNA was cloned into two expression vectors: the pSG5 mammalian expression vector for use in transcriptional studies, and the EGFP-C1 expression vector which fuses the protein C-terminal to the green fluorescent protein (GFP) cDNA, for use in protein localization studies. ORF#93 was also cloned into a VP16 activation domain construct as a component of the mammalian 2-hybrid system, to allow screening for interactions with chaperone proteins.

Using transfection assays, determine whether ORF#61 (NIP7), ORF#93 and ORF#127 influence transcription induced by ER and PR in the presence of different ligands, and in several mammalian cell lines, including breast cancer cells

The ability of ORF#93 to influence nuclear receptor function was determined by transfection into mammalian cells, including HeLa cells and T47D-YB human breast cancer

cells. At first, ORF#93 did not appear to act through modulation of receptor transcriptional activity. In the experiment shown in **Figure 7**, HeLa cells were cotransfected with PR-B and a progestin-responsive reporter (pA3-PRE_2-$TATA_{tk}$-LUC) and increasing DNA amounts of ORF#93. In this experiment, a modest increase in activity was seen in the presence of the agonist R5020 with increasing amounts of ORF#93. This effect was not seen with RU486. Similar experiments have been carried out using GR or ER and an ERE reporter, and no agonist-specific stimulation was observed. However, when the absolute effect of ORF#93 was examined, by reanalyzing the raw data, it became apparent that although ORF#93 was not a ligand-specific enhancer of PR activity, it was a general transcriptional enhancer. This is seen in **Figure 8**. In the presence of 1000ng of ORF#93 the R5020-liganded activity of PR on the luciferase reporter is almost double that of the control (no ORF#93 DNA). However, reporter activity in the dose-matched controls also increases with increasing ORF#93 amounts, suggesting that it is a general transcriptional enhancer.

Recent studies with the yeast proteins Ssn6 (another TPR domain protein) and corepressor Tup1 showed that the two proteins act together to form the repressor complex (Davie et al., 2002; Jabet et al., 2000). Therefore, transcriptional studies incorporating the corepressors SMRT and N-CoR were carried out to fully explore the possible transcriptional role of ORF#93. We have demonstrated previously that the corepressors N-CoR and SMRT suppress the partial agonist activity of tamoxifen (Jackson et al., 1997).

Since the abundance of the ORF#93 transcript was quite high in our cells we postulated that it may produce too high a background in our transfections to see any additional effect on reporter activity. Therefore, we constructed an antisense vector that knocks out expression of endogenous ORF#93 and used it to define possible decrements in PR function in the absence of this protein. Introduction of ORF#93AS into cells did not greatly affect PR transcriptional activity. However, knocking out ORF#93 opposed the SMRT suppression of tamoxifen partial agonist activity (**Figure 9**). When HeLa cells were transfected with ER and an estrogen-responsive luciferase reporter, tamoxifen increased luciferase activity to over 4-fold of untreated control levels. Cotransfection of SMRT reduced this effect by 50% and cotransfection of sense ORF#93 had little effect. However, in the presence of ORF#93AS, knocking out endogenous ORF#93 expression, SMRT no longer suppressed tamoxifen partial agonist effects and reporter activity was restored to control levels.

Perform other functional studies with expression vectors for the three clones dictated by the structural analyses

As mentioned above, the ORF#93 cDNA was cloned into the EGFP-C1 expression vector to produce a GFP-ORF#93 fusion protein. This protein can be visualized in cells under fluorescent light. The construct was then expressed in T47D-YB cells (containing PR-B) and the cells were examined for localization of the protein in the presence or absence of PR ligands. Cells were treated for one hour with 10nM R5020, 100nM RU486 or ethanol vehicle control, then fixed using cold 30% methanol/70% acetone and nuclei were visualized using DAPI which stains the nuclei. DAPI staining is blue and GFP-93 is green. In the absence of ligand, GFP-93 has a cytoplasmic localization (**Figure 10**) and exhibits a punctate expression pattern, suggestive of golgi localization. The protein appears to be excluded from the nucleus. A one-hour treatment of cells with progestin agonist or antagonist did not change the localization of GFP-93, although this is abundant time to see complete nuclear translocation of PR. To examine whether overexpression of GFP-93 inhibited translocation of PR to the nucleus, additional dual

fluorescence studies were carried out in PR-positive T47D-YB cells (**Figure 11**) in which GFP-93 was visualized green as before and PR was detected immunohistochemically and visualized red in the same cells. In untreated cells PR appeared weakly nuclear, with some cytoplasmic localization. As before, GFP-93 was located mostly in the cytoplasm. Upon treatment with R5020 or RU486, PR became tightly nuclear, and overexpression of GFP-93 did not inhibit this translocation. Furthermore, GFP-93 remained primarily cytoplasmic.

This suggests that, if ORF#93 interacts with PR intracellularly, it does so in the cytoplasm prior to PR transcriptional activation. This is consistent with what is known about TPR domain-containing proteins: these proteins act as chaperones and interact with other chaperonins such as hsp90 – another protein that binds PRs in the cytoplasm. In order to address the possibility that ORF#93 interacts with PRs as part of a multi-protein complex that includes hsp90, co-immunoprecipitation experiments were performed. **Preliminary results indicated that ORF#93 interacts with hsp90.** However, the interactions were very weak under the stringent conditions required in co-immunoprecipitation experiments. Therefore, DNA constructs were prepared in order to measure ORF#93 interactions with hsp90 under more physiological conditions. Constructs were engineered for use in mammalian two-hybrid studies. The ORF#93 cDNA was cloned as a fusion construct with the activation domain of VP16, and hsp90 cDNA was inserted into a Gal4 DNA binding domain plasmid. When cotransfected with a Gal4-RE reporter, an interaction between the two fusion proteins produces luciferase activity through the Gal4-RE reporter (**Figure 12**). Cotransfection of VP16-ORF#93 and Gal4DBD-hsp90 confirmed that ORF#93 does indeed interact with hsp90 (**Figure 13**). Furthermore, cotransfection of PR alone did not reduce the interaction. When cotransfected cells were treated with R5020 in the presence of PR-B the interaction between ORF#93 and hsp90 was enhanced. This suggested that ORF#93 may help to dissociate the chaperonin complex from PR by sequestering proteins such as hsp90. Treatment with the antagonist RU486, which is known to strongly enhance interaction between PR and hsp90, reduced the interaction between ORF#93 and hsp90 when PR was present, suggesting that PR was binding hsp90 with higher affinity and therefore making it less available to bind ORF#93.

In addition to the in vivo experiments, in vitro experiments were also performed to show the direct binding of ORF#93 to hsp90. When bacterially-expressed and purified ORF#93 and hsp90 are combined, they form a complex as shown in **Figure 14B**. To test the importance of the TPR domains in binding to hsp90, we tested proteins with point mutations of amino acids in TPR1 or TPR2. TPR repeats are degenerate 34 amino acid sequences with no position characterized by an invariant residue. However, certain amino acids are commonly observed in particular positions. Alignment of TPR sequences (**Figure 14A**) showed that lysine 13 and alanine 20, located in helix loops A and B respectively, are conserved not only within ORF#93 TPR-motifs but also in most of the TPR motifs of Hop, FKBP52, FKBP51, cyp40 and PP5 (Barent et al., 1998; Chen et al., 1994; Odunaga et al., 2003; Young et al., 1998). Therefore, these two residues were mutated to glutamic and aspartic acid in the TPR1 and TPR2 repeats of ORF#93. Both mutations of TPR1 and TPR2 abrogated ORF#93-hsp90 interaction (**Figure 14B**), suggesting that the two motifs are essential for hsp90 binding. Importantly, the three-dimensional structures of both mutants appeared to be stable and similar to ORF#93 wild type because they 1) co-migrated with ORF#93 wild type in size exclusion chromatography analysis with no signs of aggregation (not shown), and 2) retained binding to PR in a similar manner (**Figure 14C**) to the wild type.

ORF#93 mRNA expression and its progesterone regulation have also been examined. T47D-YB breast cancer cells were treated for 2 or 12 hours with 10nM R5020, 100nM RU486 or vehicle control. Cells were harvested and total RNA was isolated. 30μg of each sample was run on a denaturing agarose gel and Northern blotted using a ^{32}P-labeled ORF#93 cDNA probe. An apparent modest decrease in transcript expression, to 52% of the time matched control, was seen after 12h R5020 treatment (**Figure 15**). RU486 had little or no effect on transcript expression. Thus, **ORF#93 levels may be regulated by progesterone**.

KEY RESEARCH ACCOMPLISHMENTS:

- A full cDNA clone has been obtained for the novel DNA fragment designated ORF#93, which may be involved in nuclear receptor function.
- The genomic structure has been defined; the gene is located at 15q26.1.
- The full-length protein has been expressed.
- Interactions between ORF#93 and PR, GR and ER, have been demonstrated in vitro.
- ORF#93 is a component of PR and hsp90 complexes in cell lysates and can be incorporated into PR complexes during re-assembly with purified chaperones.
- The expression pattern of ORF#93 has been described in adult and fetal human tissues.
- The influence of ORF#93 on nuclear receptor transcriptional activity has been characterized.
- A role for ORF#93 in corepressor function has been discovered.
- In vivo localization of the ORF#93 protein has been determined; the protein is cytoplasmic and may perhaps be localized to the golgi.
- It has been demonstrated that ORF#93 binds hsp90 as well as PR-A and PR-B with high affinity.
- Antibodies (both monoclonal and polyclonal) to ORF#93 have been generated and the size of the recombinant protein has been determined.
- A direct protein-protein interaction has been demonstrated for ORF#93 and both PR isoforms in mammalian two-hybrid experiments.
- ORF#93 has been renamed CRIP100 (chaperone and receptor interacting protein, MW 100K).
- Mutational analysis of CRIP100 indicates that the TPR 1 and 2 domains of CRIP100 are required for the binding of CRIP100 to hsp90.
- A ternary complex for CRIP100, hsp90 and Hop can be isolated, suggesting distinct binding sites for CRIP100 and Hop on hsp90.
- CRIP100 binds to a novel site on hsp90 and may represent an important modulator of PR chaperoning by hsp90.

REPORTABLE OUTCOMES:

The preliminary results generated by this project have been reported in the following meeting abstracts (appended):

1. Graham JD, Abel MG, Jackson TA, Gordon DF, Wood WM, and Horwitz KB. (2000) Novel Interactors Mediating Mixed Antagonist Action on Estrogen and Progesterone Receptors in Breast Cancer. Proceedings of the Keystone Symposium: Nuclear Receptors, USA.
2. Graham JD, Abel MG, Gordon DF, Wood WM and Horwitz KB. (2000) Receptor Interacting Proteins and the Function of Progesterone and Estrogen Receptors in Breast Cancer. Proceedings of the International Congress on Endocrinology 2000, Sidney, Australia.

The results from this work have been submitted in February 2004 (appended):

Characterization of CRIP100: A Novel Tetratricopeptide Repeat Protein that Interacts with Progesterone Receptors and Hsp90 by Ahmed Chadli, J. Dinny Graham, M. Greg Abel, Twila A. Jackson, David F. Gordon, William M. Wood, David Toft, and Kathryn B. Horwitz.

CONCLUSIONS:

This project seeks to identify novel proteins that interact with antagonist-occupied steroid receptors and modify the direction of transcription. Specifically, the studies are based on the hypothesis that "mixed antagonists" such as tamoxifen, exert either more or less agonist-like activity, depending on the nature of coregulatory proteins that are recruited to the transcription complex. In the first year of this grant, we analyzed one cDNA fragment, dubbed ORF#93, that was isolated based on its ability to bind antagonist-occupied receptors. We have now cloned the full-length cDNA, defined its genomic structure, obtained a chromosome assignment, expressed the full-length protein, defined its tissue distribution and subcellular localization, and generated a polyclonal antibody that probes a 103 kDa protein. In the second year of the project functional studies have been completed. The protein does not appear to have a ligand-specific effect on PR transcription, but ORF#93 has general transcriptional effects, and antisense studies have demonstrated that the protein may also play a role in affecting corepressor actions on partial agonists. Last year we predicted that the protein may have a cytoplasmic "scaffolding" function, and serve as a matrix to allow PRs and other nuclear receptors to interact with other proteins in multiprotein complexes, perhaps in association with hsp90. We went on to demonstrate that ORF#93 does indeed interact with hsp90 and that this is influenced by the presence of PR and its ligands. Specifically, binding of ORF#93 to hsp90 involves two TPR domains located in ORF#93. It is possible that ORF#93 functions to regulate key events in the formation of nascent PR, cytoplasmic chaperone interactions and translocation to the nucleus. If so, ORF#93 may be a key protein that brings PRs into close association with cytoplasmic signaling molecules with which these receptors would otherwise not interact. For example, we have shown in other studies, that PRs interact with STATs, yet these two proteins reside in different cellular compartments. Does ORF#93 function to bring these two disparate signaling molecules together?

If so, ORF#93 may be important for cross-talk between growth factors and nuclear receptors, and we propose to test this hypothesis in future long-term studies.

REFERENCES:

Barent, R. L., Nair, S. C., Carr, D. C., Ruan, Y., Rimerman, R. A., Fulton, J., Zhang, Y., and Smith, D. F. (1998). Analysis of FKBP51/FKBP52 chimeras and mutants for Hsp binding and association with progesterone receptor, Mol Endocrinol *3*, 342-354.

Barker, S. (2003). Anti-estrogens and the treatment of breast cancer: current status and future directions, Current Opinions in Investigative Drugs *6*, 652-657.

Blatch, G. L., and Lassle, M. (1999). The tetratricopeptide repeat: a structural motif mediating protein-protein interactions, Bioessays *11*, 932-939.

Chen, M. X., McPartlin, A. E., Brown, L., Chen, Y. H., Barker, H. M., and Cohen, P. T. (1994). A novel human protein serine/threonine phosphatase, which possesses four tetratricopeptide repeat motifs and localizes to the nucleus, Embo J *18*, 4278-4290.

Crawford, D. J., Cowan, S., Fitch, R., Smith, D. C., and Leake, R. E. (1987). Stability of oestrogen receptor status in sequential biopsies from patients with breast cancer, Br J Cancer *56*, 137-140.

Davie, J., Trumbley, R., and Dent, S. (2002). Histone-dependent association of Tup1-Ssn6 with repressed genes in vivo, Molecular and Cellular Biology *22*, 693-703.

Graham, J. D., Bain, D. L., Richer, J. K., Jackson, T. A., Tung, L., and Horwitz, K. B. (2000). Nuclear receptor conformation, coregulators, and tamoxifen-resistant breast cancer, Steroids *65*, 579-584.

Gronemeyer, H., Benhamou, B., Berry, M., Bocquel, M. T., Gofflo, D., Garcia, T., Lerouge, T., Metzger, D., Meyer, M. E., Tora, L., *et al.* (1992). Mechanisms of anti-hormone action, Journal of Steroid Biochemistry & Molecular Biology *41*, 217-221.

Horwitz, K. B. (1993). Mechanisms of hormone resistance in breast cancer, Breast Cancer Res Treat *26*, 119-30.

Jabet, C., Sprague, E. R., VanDemark, A. P., and Wolberger, C. (2000). Characterization of the N-terminal domain of the yeast transcriptional repressor Tup1. Proposal for the association model of the repressor complex Tup1 x Ssn6, Journal of Biological Chemistry *275*, 9011-9018.

Jackson, T. A., Richer, J. K., Bain, D. L., Takimoto, G. S., Tung, L., and Horwitz, K. B. (1997). The partial agonist activity of antagonist-occupied steroid receptors is controlled by a novel hinge domain-binding coactivator L7/SPA and the corepressors N-CoR or SMRT, Mol Endocrinol *11*, 693-705.

Lamb, J. R., Tugendreich, S., and Hieter, P. (1995). Tetratrico peptide repeat interactions: to TPR or not to TPR?, Trends in Biochemical Sciences *7*, 257-259.

Odunaga, O. O., Hornby, J. A., Bies, C., Zimmerman, R., Pugh, D. J., and Blatch, G. L. (2003). Tetratricopeptide repeat motif-mediated Hsc-mSTI1 interaction. Molecular characterization of the critical contacts for successful binding and specificity, Journal of Biological Chemistry *278*, 6896-6904.

Young, J. C., Obermann, W. M., and Hartl, F. U. (1998). Specific binding of tetratricopeptide repeat proteins to the C-terminal 12-kDa domain of hsp90, J Biol Chem *273*.

Meeting abstract:

Presented at **Proceedings of the Keystone Symposium: Nuclear Receptors 2000, USA, 2000.**

Novel Interactors Mediating Mixed Antagonist Action on Estrogen and Progesterone Receptors in Breast Cancer.

J. Dinny Graham, M. Greg Abel, Twila A. Jackson, David F. Gordon, William M. Wood and Kathryn B. Horwitz. Division of Endocrinology, University of Colorado Health Sciences Center, Denver, Colorado 80262, USA.

The antiestrogen tamoxifen is one of the most effective treatments for estrogen receptor (ER) positive breast cancer. However, tumors inevitably develop resistance to the treatment, which we postulated is due to the emergence of inappropriate agonist-like effects of this mixed antagonist. We have shown that the balance of agonist and antagonist activities of mixed antagonists is influenced by the abundance of nuclear receptor coregulators. We demonstrated that the corepressors N-CoR and SMRT, suppress the partial agonist activities of tamoxifen and the mixed antiprogestin RU486 on ER and progesterone receptor (PR), respectively. Furthermore, a novel coactivator, L7/SPA, enhances partial agonist activity. These effects are mixed antagonist-specific, and are not observed with agonists or pure antagonists. In addition, we found that the expression levels of these coregulators may differ between tamoxifen sensitive and resistant breast tumors, suggesting that they may be determinants of tamoxifen responsiveness. We postulated that other novel factors may play a specific role in determining mixed antagonist effects in breast cancer. We have employed two different antagonist-specific screening strategies to identify proteins involved in tamoxifen and RU486 action. Conventional yeast 2-hybrid screening was performed in the presence of RU486, with the hinge and hormone binding domain of PR as bait. We have identified a novel protein of approximately 109 kDa, which interacts with PR only when liganded to RU486. The protein contains eight nuclear receptor (NR) binding LXXLL domains. Mutagenesis of one out of two NR boxes, contained in the original 2-hybrid clone, resulted in loss of PR interaction with that fragment. The protein also contains three putative tetratricopeptide repeat domains, which may be involved in nuclear targeting of RU486-liganded PR and act as a scaffold for assembly of PR into multiprotein complexes. Recent evidence suggests that mixed antagonist-specific interactions with ER and PR involve multiple contacts with both AF-1 and AF-2 of the intact receptors. To screen for such proteins we have used a Sos recruitment 2-hybrid screening strategy with a full length ER bait, in the presence of tamoxifen. A number of antagonist-specific ER interacting proteins have been isolated and will be described.

Meeting abstract:

Presented at **Proceedings of the International Congress on Endocrinology 2000, Sydney, Australia, 2000.**

Receptor Interacting Proteins and the Function of Progesterone and Estrogen Receptors in Breast Cancer.

J. Dinny Graham, M. Greg Abel, David F. Gordon, William M. Wood and Kathryn B. Horwitz, Division of Endocrinology, University of Colorado Health Science Center, Denver, Colorado 80262, USA.

The nuclear receptors for estrogen and progesterone (ER and PR) are important therapeutic determinants in breast cancer. Tumors expressing both receptors are generally well differentiated, indolent, and likely to respond to treatment with the mixed antiestrogen, tamoxifen. However, responsive tumors inevitably become tamoxifen-resistant and progress, often in the face of continued ER expression. We postulated that this is due to an increase in the partial agonist activity of tamoxifen. To test this hypothesis we have been searching for novel proteins that interact with receptors and modify the activities of mixed antagonists like tamoxifen. Using mixed antagonist-biased interaction screening, we have identified proteins that interact with ER and PR, and regulate transcription. The corepressors N-CoR and SMRT suppress the partial agonist activities of tamoxifen and the antiprogestin RU486, whereas the coactivator L7/SPA enhances this activity, yet has no effect on pure agonists or antagonists. In tamoxifen-resistant tumors removed from patients, we see a trend towards decreased expression of corepressors. In the same screen we identified a cDNA fragment encoding a novel protein, that we have now cloned and fully sequenced. The 109 kD protein interacts best with unliganded and mixed antagonist-bound PR, and less well with agonist-bound PR. The 944 amino acid protein sequence contains four nuclear receptor interaction LXXLL motifs. Additionally, there are three tetratricopeptide repeat (TPR) motifs in the N-terminus, characteristic of chaperonin/immunophilin binding proteins. Indeed, hsp90 also interacts with the protein strongly in protein interaction experiments. When expressed as a green fluorescent fusion protein, it shows a punctate cytoplasmic localization, which persists in the presence of progestins. We are testing the hypothesis that this protein has a scaffolding function, and plays an integral role in the correct expression and folding of nascent receptors, and perhaps their subcellular localization.

Manuscript abstract (submitted to the Cold Springs Harbor Symposium on Chaperones):

Characterization of CRIP100: A Novel Tetratricopeptide Repeat Protein that Interacts with Progesterone Receptors and Hsp90

Ahmed Chadli[1], J. Dinny Graham[2], M. Greg Abel[2], Twila A. Jackson[2], David F. Gordon[2], William M. Wood[2], David Toft[1] and Kathryn B. Horwitz[2]

[1]Department of Biochemistry and Molecular Biology, Mayo Clinic, Rochester, MN
[2]Department of Endocrinology, University of Colorado Health Science Center, Denver, CO

The chaperoning and maturation pathway of the progesterone receptors (PRs) is an ordered and coordinated molecular event involving a number of chaperones and co-chaperones. Transcriptional regulation by the PRs is also a tightly controlled process that is dependent on associations with other cellular proteins. However, the mechanisms for these processes remain unclear and missing regulatory factors are yet to be discovered. In this report we describe a new PR and hsp90 co-factor called CRIP100 (chaperone and receptor interacting protein, MW 100K). CRIP100 is a 103 kDa, monomeric protein containing three TPR motifs and four LXXLL sequences. The protein binds both PRs and hsp90 in mammalian two-hybrid assays and has a cytoplasmic localization with a weak transcriptional enhancing effect on PRs. CRIP100 is a component of PR and hsp90 complexes in cell lysates and can be incorporated into PR complexes during re-assembly in vitro in reticulocyte lysate or with purified chaperones. CRIP100 interacts directly with both isoforms of PR (A and B) and with hsp90 with high affinity and these interactions are concentration- and temperature-dependent. TPR motifs in CRIP100 are essential for hsp90 binding, but surprisingly, Hop, previously shown to interact with the C-terminal TPR recognition motif of hsp90, does not compete with CRIP100 for hsp90. A ternary complex of CRIP100, Hsp90 and Hop can be isolated, suggesting distinct binding sites for CRIP100 and Hop on hsp90. Remarkably, CRIP100 binds fragment 1-332 of hsp90 indicating that a second TPR recognition site exists in the N-terminal domain of hsp90. Thus, CRIP100 binds to a novel site on hsp90 and may represent an important modulator of PR chaperoning by hsp90.

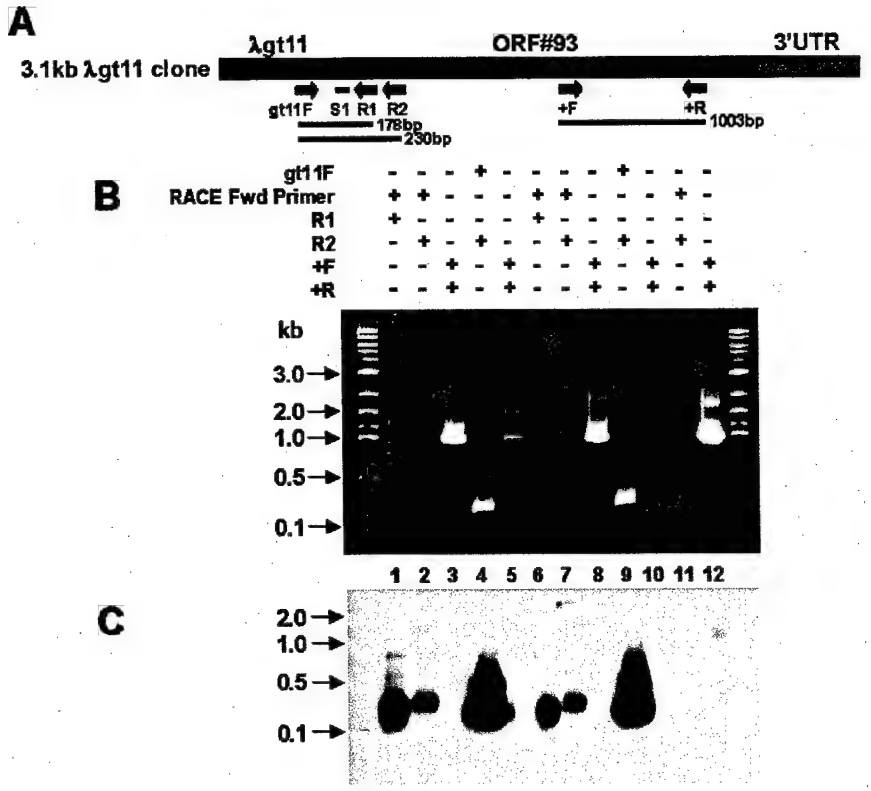

Figure 1: 5'RACE analysis of an ORF#93 clone retrieved from a screening of the λgt HeLa cell cDNA library. A. Location of oligos (gt11F, S1, R1, +F, and +R) used for the analysis. B. PCR amplification of a vector containing the ORF#93 insert. DNA bands were visualized on an ethidium bromide-stained gel. C. Southern blot analysis of PCR products using the S1 oligo as a probe.

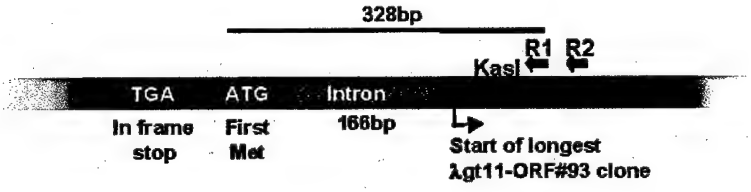

Figure 2: Genomic structure of ORF#93.

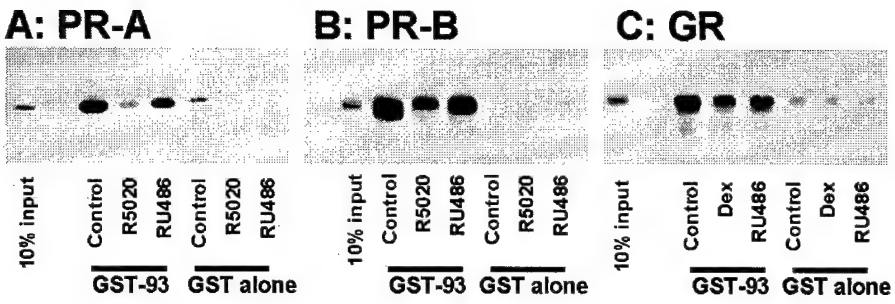

Figure 3: GST pull-down assays using GST-ORF#93. PR-A, PR-B and GR were transfected into HeLa cells. Aliquots of whole cell extracts were incubated with GST-93-bound sepharose or GST alone-bound sepharose. The strongest binding was observed for unliganded or antagonist-bound PR and GR.

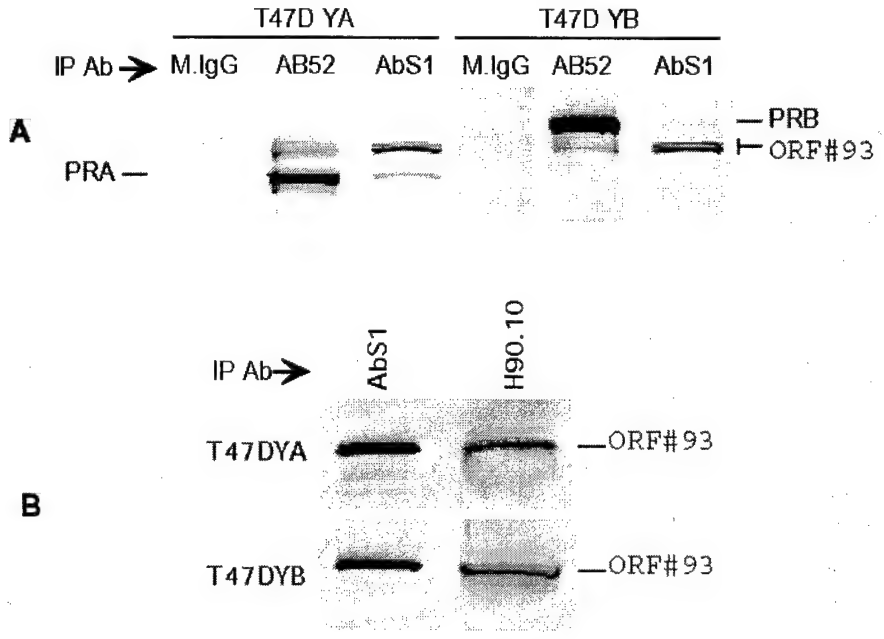

Figure 4: Co-immunoprecipitation of PR-A, PR-B, and ORF#93. A. Cell lysates containing only PR-A (T47D YA) or PR-B (T47 YB) were incubated with antibodies: AB52 (PR-A and PR-B), AbS1 (ORF#93) or control (M.IgG). Immunoblots indicate PR-A clearly co-precipitates with ORF#93, while PR-B was barely detectable. B. Binding of ORF#93 to hsp90 (using H90.10 antibody) is clearly shown, whether the ORF#93 or hsp90 antibody is used for immunoprecipitation.

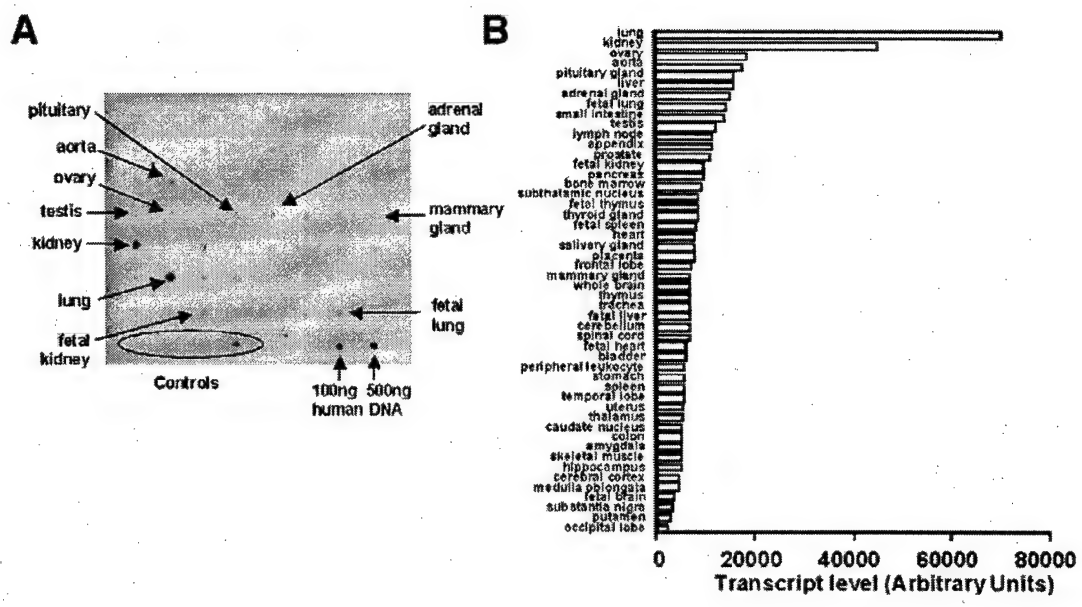

Figure 5: Multi-tissue RNA blot analysis using ^{32}P-dCTP-labelled ORF#93. The blot contains equal amounts of RNA from 43 adult human tissues, seven fetal tissues and eight controls, including yeast, E. coli, human RNA and human DNA. Results were visualized on the phosphorimager and quantified densitometrically. The strongest expression was seen in lung and kidney. Expression was clearly detectable in potential nuclear receptors targets, including the ovary, testis, adrenal, pituitary, and mammary glands.

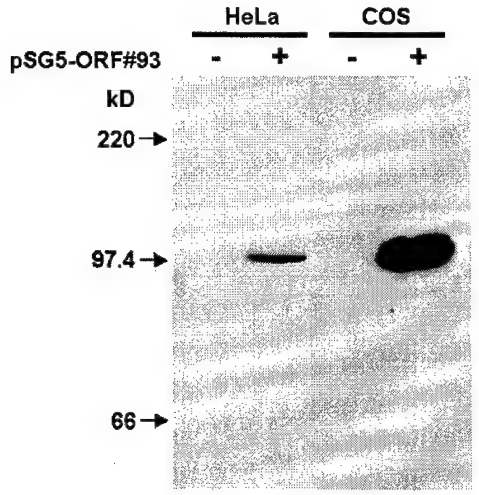

Figure 6: Western blot analysis of HeLa and COS cells for ORF#93. A poluclonal antibody to ORF#93 was able to detect ORF#93 in HeLa and COS cells that were transfected with the pSG5 expression vector containing ORF#93.

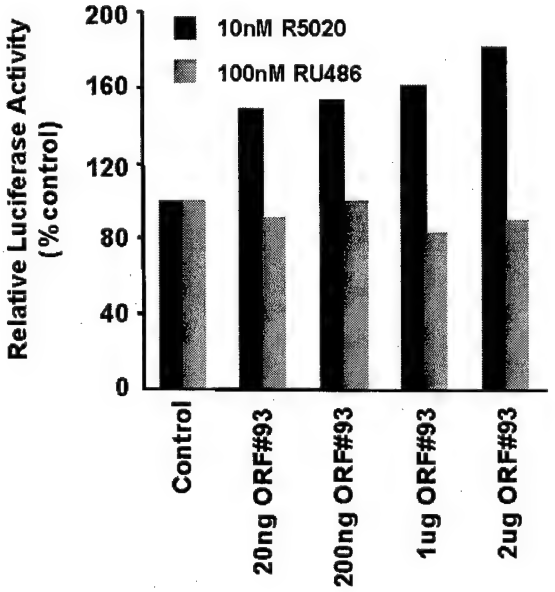

Figure 7: Effect of ORF#93 on the transcriptional activity of PR-B. HeLa cells were transfected with a PR-B expression vector and a PRE_2-$TATA_{tk}$-luciferase reporter, in the presence of increasing amounts of ORF#93. About 18h after transfection, the cells were treated with R5020, RU486 or ethanol vehicle, then harvested 24h later. ORF#93 caused a modest, dose-dependent increase in agonist-reporter activity and had no effect on partial agonist activity of RU486.

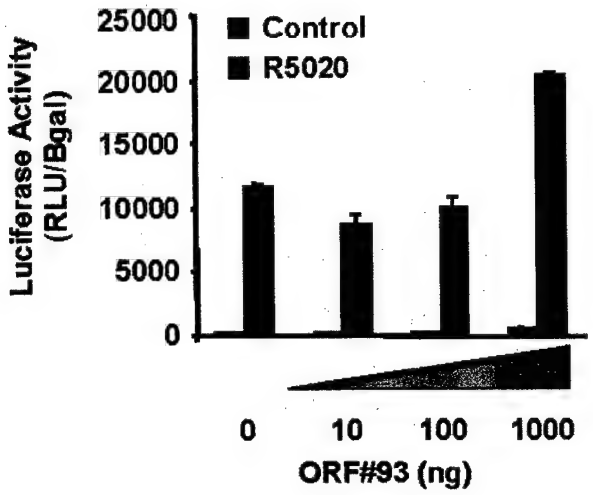

Figure 8: Effect of ORF#93 on the R5020-liganded activity of PR-B. R5020-liganded PR-B activity nearly doubled on a luciferase reporter at a 1000ng dose of ORF#93 as compared to the no DNA dose of ORF#93. Reporter activity in dose-matched controls also increase with increasing ORF#93, suggesting that it is a general transcriptional enhancer.

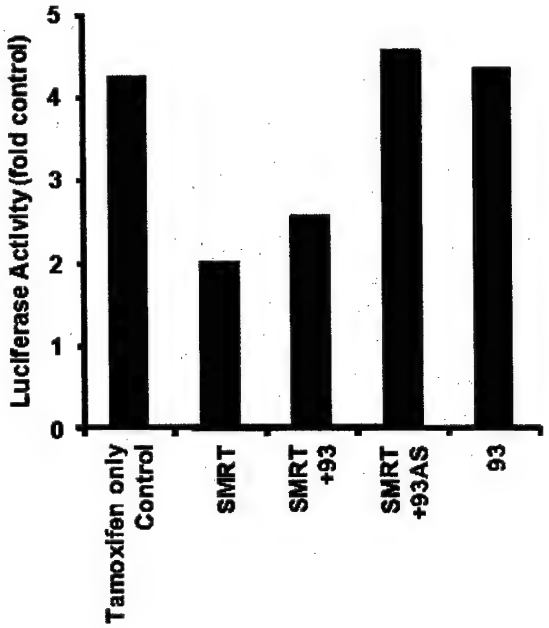

Figure 9: Effect of SMRT and ORF#93 on the transcriptional activity of tamoxifen-bound PR-B. The presence of ORF#93 did not appear to affect PR transcriptional activity. In the presence of ORF#93AS, which knocks out endogenous ORF#93 expression, SMRT is no longer able to suppress the effects of tamoxifen.

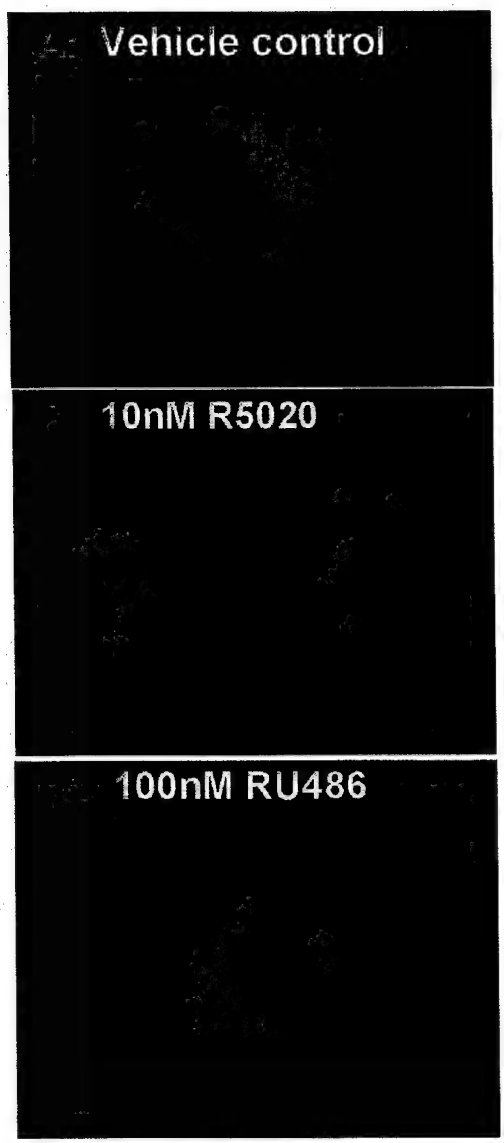

Figure 10: Localization of GFP-93 in T47D YB cells treated by an ethanol vehicle control (A), 10 nM R5020 (B), and 100 nM RU486. 24h after transfection, the cells were treated with R5020, RU486 or vehicle for 1h, then fixed in 70% acetone, 30% methanol. Nuclei were visualized using DAPI (blue), while GFP-93 is visualized in green. GFP-93 had a cytoplasmic localization, even in the presence of ligands.

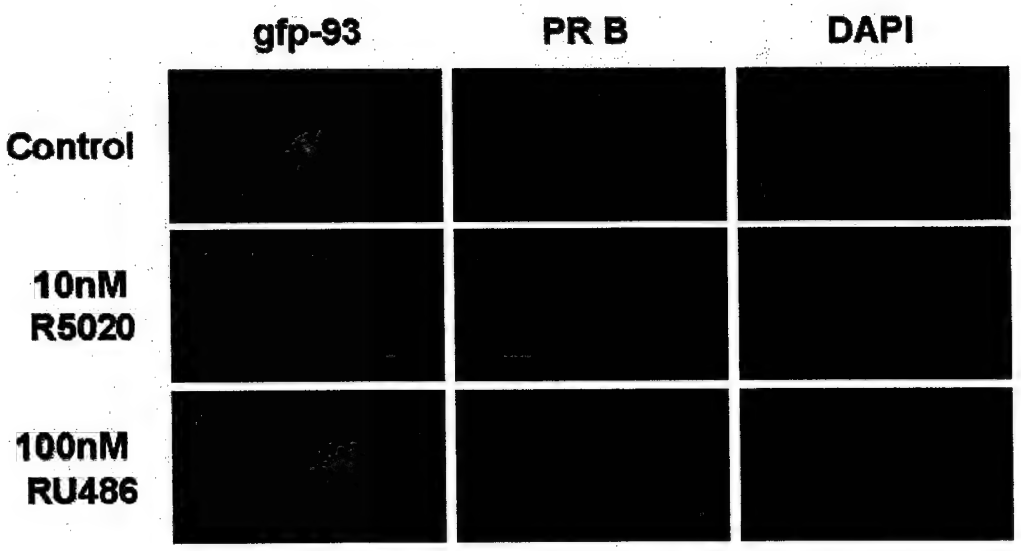

Figure 11: Localization of GFP-93 in untreated and treated T47D-YB cells. In untreated cells, PR-B appeared to be present in both the nucleus and cytoplasm, while GFP-93 was predominantly cytoplasmic. Upon treatment with R5020 or RU486, PR-B became completely nuclear. Overexpression of GFP-93, which remained in the cytoplasm, did not inhibit the translocation of PR-B into the nucleus.

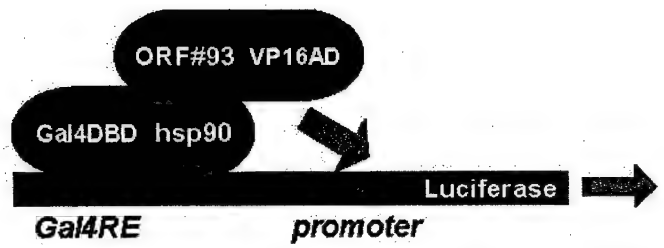

Figure 12: Schematic of the constructs used in mammalian two-hybrid studies. ORF#93 cDNA was cloned as a fusion construct with the activation domain of VP16. hsp90 cDNA was inserted into a Gal4DBD plasmid. When cotransfected with a Gal4-RE reporter, luciferase activity will be produced if an interaction between the two fusion proteins occur.

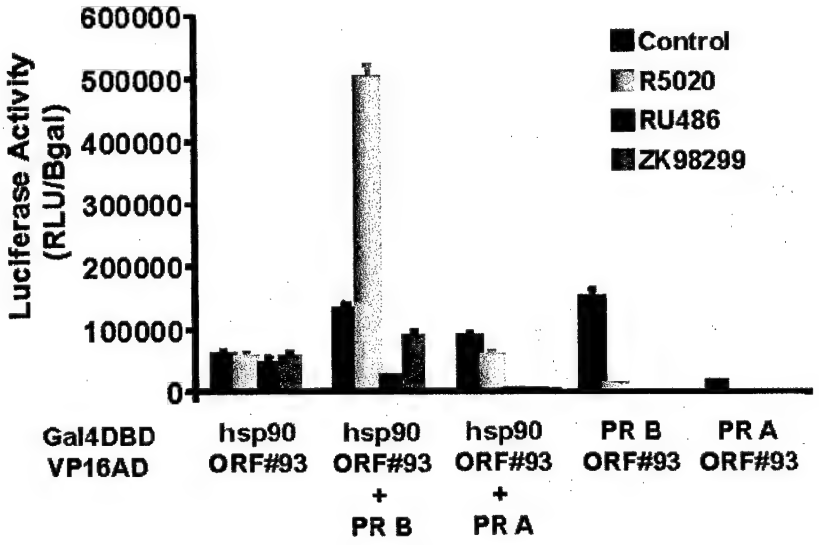

Figure 13: Results from mammalian two-hybrid experiments. Cotransfection of VP16AD-ORF#93 and Gal4DBD-hsp90 show that ORF#93 does interact with hsp90. Cotransfection of PR alone did not reduce the interaction. When cotransfected cells were treated with R5020 in the presence of PR-B, the interaction between ORF#93 and hsp90 was enhanced. Treatment with RU486 reduced the interaction with ORF#93 and hsp90 when PR was present.

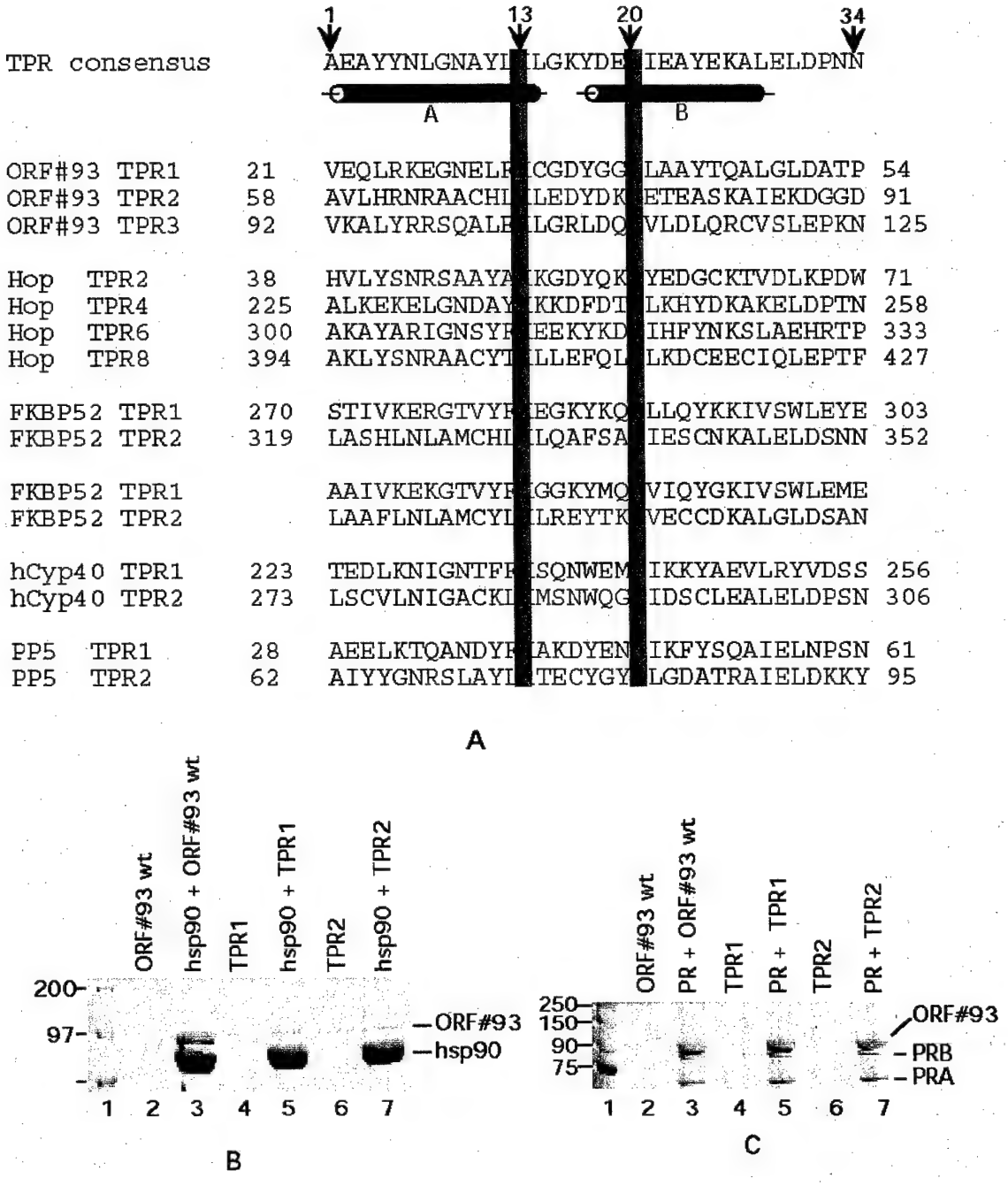

Figure 14: A. Sequence alignment of TPR motifs from ORF#93, Hop, FKBP52, hCyp40, and PP5. Highlighted in red are the highly conserved lysine and alanine residues. B. Wild-type ORF#93 is able to bind hsp90 (lane 3), whereas mutation of either TPR1 (lane 5) or TPR2 (lane 7) of ORF#93 eliminates its interaction with hsp90. C. Binding of PR-A and PR-B to ORF#93 is retained in all cases.

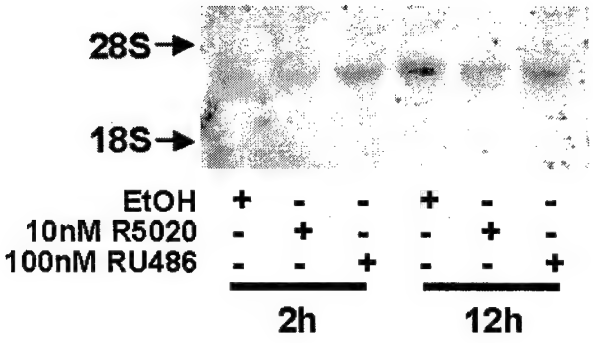

Figure 15: Northern blot analysis of ORF#93 mRNA expression and its regulation by progestins. T47D-YB cells, treated for 2 or 12 hours with R5020, RU486 or vehicle control were harvested and total RNA was isolated. 30μg of each samples was run on a denaturing agarose gel and probed with ^{32}P-labelled ORF#93 cDNA. A modest 52% decrease in transcript expression was seen after 12h R5020 treatment. RU486 had little or no effect on transcript expression.

Abstract

The chaperoning and maturation pathway of the progesterone receptor (PR) is an ordered and coordinated molecular event involving a number of chaperones and co-chaperones. Transcriptional regulation by the PR is also a tightly controlled process that is dependent on associations with other cellular proteins. However, the mechanisms for these processes remain unclear and missing regulatory factors are yet to be discovered. In this report we describe a new PR and hsp90 co-factor called CRIP100 (chaperone and receptor interacting protein, MW 100K). CRIP100 is a 103 kDa, monomeric protein containing three TPR motifs and four LXXLL sequences. The protein binds both PR and hsp90 in mammalian two-hybrid assays and has a cytoplasmic localization with a weak transcriptional enhancing effect on PR. CRIP100 is a component of PR and hsp90 complexes in cell lysates and can be incorporated into PR complexes during re-assembly in vitro in reticulocyte lysate or with purified chaperones. CRIP100 interacts directly with both isoforms of PR (A and B) and with hsp90 with high affinity and these interactions are concentration- and temperature-dependent. TPR motifs in CRIP100 are essential for hsp90 binding, but surprisingly, Hop, previously shown to interact with the C-terminal TPR recognition motif of hsp90, does not compete with CRIP100 for hsp90. A ternary complex of CRIP100, Hsp90 and Hop can be isolated, suggesting distinct binding sites for CRIP100 and Hop on hsp90. Remarkably, CRIP100 binds fragment 1-332 of hsp90 indicating that a second TPR recognition site exists in the N-terminal domain of hsp90. Thus, CRIP100 binds to a novel site on hsp90 and may represent an important modulator of PR chaperoning by hsp90.

Introduction

Throughout its functional life, the activities of the progesterone receptor (PR) are inseparably linked to its associations with other proteins that are essential for normal progesterone action. Nascent unliganded PR is associated with a multi-functional complex of proteins, which includes the heat shock proteins hsp70 and hsp90 plus several co-chaperone proteins. This heterocomplex is responsible for correct assembly and folding of the newly synthesized PR as well as preventing its degradation (1). Recent studies indicate additional roles of molecular chaperones in receptor trafficking and in the maintenance of receptor function in the nucleus (2,3). Dissociation of PR from the chaperone complex occurs at the time of ligand binding . This causes a conformational change and dimerization, resulting in association of the progestin-complexed PR dimer with specific coactivators and general transcription factors and binding to progestin response elements (PREs) in the promoters of target genes (4-8).

Chaperoning and activation of the progesterone receptor (PR) are complex processes involving the coordinated actions of molecular chaperones assisted by several co-chaperones (1,9,10). Cell free systems, using reticulocyte lysate or a purified protein system containing hsp90, hsp70, hsp40, Hop and p23, have been of crucial importance in dissecting this ordered pathway that leads to the hormone-responsive state of the receptor (1,9,10). This hsp90 chaperoning pathway is thought to be initiated by hsp40 binding to PR (11). The early complex of hsp40/PR is able to bind hsp70, then hsp90 and the co-chaperone Hop. The Hop in this intermediate complex would be replaced by one of the immunophilins (FKBP51, FKBP52, and cyp40) in mature complexes that also bind the co-chaperone p23 and are able to bind hormone (12). This late event is thought to induce a conformational change of the receptor triggering its dissociation from molecular chaperones and its dimerization. These ligand-induced conformational changes also affect the

ability of the receptor to recruit co-activator or co-repressor molecules and consequently determine its ability to activate or repress transcription of target genes (8,13).

Although the overall mechanism might be as described above, details and dynamics of this process are still unclear. For instance, mechanisms for the exchange of different associated proteins are mostly unknown. Furthermore, several additional proteins have been discovered recently that interact with hsp90 or hsp70 such as Chip, Bag1, TPR2 and Aha1 (1,9,10,14,15). These are all likely to have important roles in some aspect of the hsp70/hsp90 chaperoning process to provide a more complex and versatile process than that described above.

There are also a number of proteins that interact with the PR to act as co-regulators of PR activity (8) or to relate PR functions with other cell signaling pathways (16,17). We describe here a novel protein, CRIP100, that interacts with both PR and with hsp90 in two-hybrid analysis. Expression of CRIP100 provides a slight enhancement in PR activity, but it does not appear to be a co-activator. The interactions of CRIP100 with hsp90 and PR are direct and involve separate domains of CRIP100. The binding of hsp90 involves a TPR domain on CRIP100; however, this interacts with an N-terminal site on hsp90 rather than the known TPR binding site at its C-terminus.

Materials and Methods

Yeast two-hybrid screen: The yeast two-hybrid screen was described previously (18). The plasmid pLEXA:H-HBD was transformed into the Saccharomyces cerevisiae reporter strain L40 (Mata his3D200 trp1-901 leu2-3 112ade2 LYS2::(lexAop)$_4$-HIS3 URA3::(lexAop)$_8$-lacZ GAL4 gal80) to yield the L40-LEXA:H-HBD strain. This strain was transformed with a library of HeLa cell cDNAs fused to the GAL4 activation domain in the CRIPGH vector (Clontech, Palo Alto, CA) and plated on selective media containing 10mM RU486. Interacting clones were detected by growth on histidine drop-out plates and confirmed by b-galactosidase assay.

GST pull-down: The CRIP100 cDNA was sub-cloned into pGEX-4T-1 (Promega) and expressed in BL-21 codon + E. coli (Stratagene, LaJolla, CA) as a C-terminal fusion to glutathione S-transferase. Crude bacterial extracts were prepared by sonication in PBS containing 1% triton X-100, 2.5 mM DTT, 10% glycerol, 0.5mM PMSF, and complete protease inhibitors (Roche) at 4°C, followed by centrifugation 10,000 rpm, 10 minutes at 4°C. Supernatants containing CRIP100 or gst alone were bound to glutathione sepharose 4B (Amersham-Pharmacia Biotech) at 4°C, for 1 hour. The sepharose slurry was washed three times with binding buffer (20mM HEPES, pH 7.9, 60mM NaCl, 0.1mM EDTA, 6mM MgCl2, 1mM DTT, 0.5mM PMSF, 10% glycerol, complete protease inhibitor), then incubated with HeLa whole cell extracts containing transfected PR A, PR B or GR, 2 hours at 4°C. Where indicated, samples were incubated in the presence of 10nM R5020, 100nM RU486, 10nM dexamethasone or ethanol vehicle. In this instance, the PR or GR transfected HeLa cells had also been exposed to the same treatment for 1 hour prior to harvesting and preparation of whole cell protein extracts. Samples were washed twice with binding buffer containing 0.05% NP-40, and twice with binding buffer alone. The sepharose pellets were resuspended in SDS-PAGE loading buffer and heated to 100°C for 3-5

minutes. Bound proteins were separated on denaturing 7.5% polyacrylamide gels and visualized by immunoblotting, using antibodies to PR and GR.

Detection of CRIP100 protein in tissues and cell lines: Cytosols from different tissues and cells were made using the following buffer: 10mM Tris, 50mM KCl, 10mM monothioglycerol, 5mM EDTA, protease inhibitors (Roche). To detect the protein in the cytosol, 30 μg of cytosolic proteins were loaded on the gel. Immunoprecipitations (IP) were carried out using 800 μg proteins from rat brain and cell lines cytosols and 5 μl monoclonal antibody CRIP100#2 ascites coupled to 12.5μl protein G resin. Mixtures were incubated for 30 min at 30°C. Resins were washed 4 x 1 ml of above indicated buffer without protease inhibitors supplemented with 0.01% NP40 and bound proteins were eluted with sample buffer, resolved on denaturing 10% polyacrylamide gel, transferred onto PVDF membrane and detected with CRIP100#2 at 1/5000 dilution.

Cell culture and transcription assays: The T47Dco and T47D-Y breast cancer cell lines were generated in our laboratory and have been described previously (19,20). HeLa cervical carcinoma cells were obtained from the ATCC, Manassas, VA. Cells were maintained as continuous monolayer cultures in modified Eagle's medium (MEM) supplemented with 6ng/ml insulin (Invitrogen-Gibco BRL) and 5% fetal bovine serum (FBS, Hyclone Laboratories, Logan, UT) at 37°C and 5% CO_2. For transfections, HeLa cells were plated at 2 x 10^5 cells/10cm dish or 1.2 x 10^5/6cm dish, in phenol red-free MEM containing 5% charcoal-stripped FBS one day prior to transfection. Transient transfections were carried out using a standard calcium phosphate precipitate-mediated method. Cells were exposed to precipitates, containing a total of 20 mg DNA per dish, for 16 to 20 hours. Precipitates were then removed, monolayers were washed

with serum-free medium and hormones were added to the cells for 24h, in fresh medium containing 7.5% charcoal-stripped FBS. The cells were harvested, lysed in a detergent buffer, then b-galactosidase and luciferase activities were measured.

Immunohistochemistry: T47D-YB cells were plated onto coverslips in culture dishes at 4 x 10^5 cells per 6cm dish. The cells were transfected with the pEGFP-C1-93 construct, containing the CRIP100 cDNA fused C-terminally to green fluorescent protein. Two days after transfection, the cells were washed with PBS, and fixed in ice cold 70% acetone-30% methanol. Non-specific binding was blocked using 10% normal goat serum in PBS, 1 hour at room temperature. Cell nuclei were stained using DAPI reagent at 1:10,000 in methanol, 20 minutes at room temperature. After washing PR B was visualized by incubation with the AB-52 monoclonal antibody to PR, at 1:50 dilution, 2 hours at room temperature, followed by rhodamine-conjugated anti-mouse secondary (1:500, 1 hour, room temperature).

Mammalian 2-hybrid: Interactions between CRIP100, hsp90 and PR A and B were measured in the Mammalian Matchmaker 2-hybrid system (Clontech, Palo Alto, CA). In this system hsp90 and PR A and B were sub-cloned into the pM vector and expressed as fusions with the DNA binding domain of Gal-4. CRIP100 and PR A and B were sub-cloned into pVP16AD and expressed as VP16 activation domain fusion proteins. Combinations of the pM and pVP16AD fusion constructs were co-transfected into HeLa cells with a Gal4-tk-luciferase reporter construct containing two Gal-4 response elements upstream of the thymidine kinase promoter and luciferase gene, and interactions were quantitated by measurement of luciferase activity.

CRIP100 expression and purification: A system for CRIP100 expression in E. coli has been described. Bacteria were grown to 0.6 absorbance at 600 nm and induced with 0.5 mM IPTG for 2h at room temperature. Cells from 1 liter of culture were re-suspended 20 ml Buffer A (10 mM Tris, 50 mM KCl, 0.01% NP40, 10 mM monothioglycerol) supplemented with protease inhibitors (0.1 mM leupeptin/0.1 mg/ml bacitracin/77 μg/ml aprotinin/1.5 μM of pepstatin/1 mM 4-(2-aminoethyl) benzensulfonyl fluoride). Cells were then lysed by sonication and the lysate was clarified by ultracentrifugation (100,000 g) for 45 min. The supernatant was loaded on a glutathion-Sepharose column equilibrated with Buffer A. Unbounded protein was washed out and GST-CRIP100 was eluted with Buffer A containing 10 mM glutathion.

To prepare CRIP100, the GST was cleaved by thrombin (3U/mg of GST-CRIP100, Sigma) in Buffer A supplemented with 2.5% glycerol. The mixture was incubated for 2 hours at 25C. After cleavage, some aggregation of the protein was observed and removed by centrifugation. Free GST was removed by recycling the solution on glutathione-Sepharose equilibrated with Buffer A supplemented with 2.5% glycerol. The flowthrough material, containing CRIP100 and thrombin was collected and concentrated to 0.5 ml by ultrafiltration (Vivascience). CRIP100 and thrombin were separated by size exclusion chromatography on Superdex 200.

Protein purification: Human hsp90 beta was overexpressed in SF9 cells and purified from cell lysates by chromatography on DEAE-cellulose, heparin-agarose, MonoQ and Superdex as described previously (21). The preparation was 99% pure as assessed by densitometry of SDS/PAGE gels. Hsp70, Ydj, Hop and p23 were expressed and purified as described previously (22).

Monoclonal antibody production: Purified CRIP100 was used to produce a mouse monoclonal IgG antibody named AbS1 using conventional methods (23).

Size exclusion chromatography: A Superdex 200 column (10/10, Pharmacia-Biotech) was equilibrated with 10 mM Tris, pH 7.5, 100 mM KCl, 2 mM DTT, and 1 mM EDTA. Elution was performed using the same buffer at a flow rate of 0.5 ml/min and proteins were detected by the UV absorbance. The column was calibrated with thyroglobulin (669 kDa), ferritin (440 kDa), catalase (232 kDa), aldolase (158 kDa), BSA (67 kDa) and chymotrypsinogen A (25 kDa) (Pharmacia Biotech).

Immunoprecipitation: Pellets (25 µl) of protein A-Sepharose containing bound antibody as indicated were resuspended in 200 µl of incubation buffer (10 mM Tris-HCl, 50 mM KCl, 5 mM $MgCl_2$, 2 mM DTT, 2.5% glycerol, pH 7.5 at 25C) containing the proteins of interest. Incubations at 30C were done in heated water baths, with resuspension of the samples every five minutes. Samples were subsequently washed four times with 1 ml of incubation buffer by centrifugation (at 4C) and resuspention. The samples were analyzed by SDS-PAGE on 10% gels. The gels were stained with Coomassie blue or transferred to PVDF membranes for immunodetection with specified antibodies.

Progesterone receptor complex assembly in reticulocyte lysate: ^{35}S-methionine-labeled CRIP100 was prepared by in vitro translation using the TnT system (Promega). The translation solution was supplemented with regeneration system (10 mM phosphocreatin) (ditris salt, Sigma) and creatin phosphokinase (3.5 units/100 µl of lysate; type I, from rabbit muscle, Sigma). One hundred µl sample of translation solution was incubated with immuno-resin with or without PR.

Resins were incubated for 30 min at 30C in water bath with suspension of the samples every five minutes. Sample was washed 5 times with 1 ml of buffer A. Bound proteins were resolved on 10% SDS-PAGE, transferred to PVDF membrane (Millipore, Massachusetts) and the radioactivity was assessed using a storm 840 phosphoimager (Molecular Dynamics, New Jersey).

Progesterone receptor complex assembly with purified proteins: Progesterone receptor (PR) from chick oviduct was adsorbed onto PR22 antibody-protein A-Sepharose and was assembled into complexes as described by Kosano et al. (22). The incubation contained ~.0.05 μM PR plus 1.4 μM hsp70, 0.8 μM hsp90 dimer, 0.2 μM Ydj-1, 0.08 μM Hop plus 2.6 μM p23. The samples also contained 20 mM Tris, pH 7.5, 5 mM $MgCl_2$, 2 mM dithiothreitol, 0.01% Nonidet P-40, 50 mM KCl and 5 mM ATP. Unless stated otherwise, after incubation for 40 min. at 30C, 0.1 μM [^{3}H] progesterone was added for incubation on ice for 3 h. The complexes were then isolated and assessed for bound progesterone and for protein composition.

Site direct mutagenesis: The pT28a-hCRIP100 plasmid was used as a template for the generation of double amino-acids substitutions mutants using the QuickChange site-directed mutagenesis kit (Stratagene, La Jolla, CA). In TPR1 motif the residue Lysine 13 was changed to glutamic acid and residue alanine 20 changed to aspartic acid. In TPR2 motif, both residues were changed to glutamic acid. In the four NR motifs, leucine residues 1 and 2 were changed to serines. All mutants clones were sequenced to confirm the mutations and the authenticity of the remaining CRIP100 sequence.

Cytosol preparation and immunoprecipitation: Cells or tissues were harvested and lysed in buffer A with protease inhibitors. Cytosols were cleared by centrifugation (100.000), 45 min and used for immunoprecipitations of PR complexes, hsp90 complexes or CRIP100 using antibodies AB52, PR6 or MC243 for PR, H9010 for human hsp90 and AbS1 for CRIP100. Immunoprecipitation reactions were carried out by incubation of immunoresins with the cytosol for 90 min in ice or 30 min at 30C. Nonspecific proteins were removed by washing the resins 5 times with binding buffer. Bound proteins were eluted with sample buffer, resolved by 10% SDS-PAGE and transferred to PVDF membrane. Proteins were then detected by western blotting with the appropriate antibody.

Quantification of protein levels: Arbitrary densitometric values (AU) for the indicated bands were obtained by using IP lab Gel 1.5e software (Signal Analytics, Virginia).

Evaluation of Hsp90/CRIP100 affinity

The mean AU values were converted to μM equivalent by normalizing them against 1 μg samples of CRIP100 run on the same gel. To obtain the values of free CRIP100, the amount of bound CRIP100 was subtracted from the initial amount added to the sample. The Scatchard plot is linear with an equation $Y = -22.9 \times +0.5951$ corresponding to a Kd = 43 nm with the scatter illustrated by an $R2 = 0.9914$.

Results

Cloning and characterization of a novel PR-binding protein: A construct containing the hinge and hormone binding domain of PR was used in a yeast 2-hybrid screen in the presence of the mixed progestin antagonist RU 38486 (18). By this method a number of antagonist-specific PR-

interacting proteins were discovered, including a novel 1kb clone called CRIP100. In subsequent screening the candidate interacted with the PR bait only when RU486 was present, suggesting that it may be involved in antagonist-specific effects. Confirmation of the interaction is shown in Fig.1. The CRIP100 C-terminal fragment interacted specifically with the PR hinge-HBD bait. In the yeast 2-hybrid verification shown in Figure 1A, transformed yeast were grown on selective media containing either RU486 or ethanol vehicle control. Cotransformation of the cells with the PR hinge-HBD bait and the CRIP100 C-terminal clone relieved growth suppression in the presence of RU486, but not with vehicle (Fig 1A, segment 1). No growth was observed when cells were transformed with either CRIP100 or the PR bait alone (Fig. 1A, segments 4 and 5, respectively) or when the CRIP100 clone was cotransformed into cells with a lamin-bait vector control (Fig. 1A, segment 2). Cells transformed with the commercially supplied positive control (Fig. 1A, segment 6) or with a ligand-independent constitutively active library clone (Fig. 1A, segment 3) grew on the selective media in both the presence and absence of RU486.

To further confirm the interaction between CRIP100 and PR or other steroid hormone receptors, the full-length CRIP100 product was expressed as a fusion protein with glutathione S-transferase (gst)and used in gst pull-down experiments with whole cell extracts containing over-expressed PR A, PR B or glucocorticoid receptor (GR). Products were separated on denaturing polyacrylamide protein gels and immuno-blotted for PR or GR. The gst-CRIP100 fusion interacted with both PR A and B, as well as GR (Fig.1B). All three nuclear receptors strongly bound the protein in gst pull-down, in the absence of ligand. A decrease in binding with receptor was seen when the mixed antagonist RU486 was present and even weaker binding was detected in presence of the receptor agonist R5020. No binding was observed between the receptors and gst alone.

The full length CRIP100 gene was cloned by cDNA library screening and 5'-RACE. In subsequent searches of the database, the CRIP100 genomic sequence was found as part of a disorganized BAC clone. Analysis of the full genomic sequence against the cDNA showed that the gene is made up of XXX exons, giving rise to an approximately 3.3 kilobase transcript, encoding a 944 amino acid protein (schematic, Fig.1C) with a predicted molecular weight of 103 kDa. The gene contains three putative tetratricopeptide repeat (TPR) domains at the N-terminal end of the protein. These motifs are involved in protein-protein interactions in a diverse range of molecules (24). The sequence also contains four LXXLL motifs, referred to as NR-boxes in transcriptional coregulators and responsible for binding nuclear receptors (13,26).

Expression and cell localization of CRIP100: The CRIP100 transcript was ubiquitously expressed, although at low levels (Fig.2A). Probing a northern blot of total RNA from HeLa cervical carcinoma cells and T47Dco breast cancer cells revealed a single RNA species, with a mobility close to the predicted 3.3kb (Fig.2A, inset). Detection on a multiple human tissue RNA blot indicated broad expression of the transcript, with highest expression seen in the lung and kidney. Signal was also detected in progestin target tissues such as the ovary and mammary gland (uterine tissues were not represented on the blot). This result was also confirmed by protein immunoblotting. A monoclonal antibody to CRIP100 was produced and used to detect the protein in cytosols of rodent tissues and human ovarian cell lines (Fig.2B). Among the tissues examined, highest expression of CRIP100 was seen in mouse lung, kidney, liver, spleen and uterus. The protein was also present in tongue, brain and testis, and was lowest in heart and skeletal muscle cytosols. Expression of CRIP100 was also seen in human ovarian cancer cell line cytosols and was enriched by immunoprecipitation.

To determine the cellular localization of CRIP100 the protein was expressed as a fusion with green fluorescent protein (gfp-CRIP100). The gfp-CRIP100 construct was transiently transfected into T47D-YB breast cancer cells, which express high levels of PR B. The cells were then treated with R5020, RU486 or vehicle, fixed, and PR was visualized immunohistochemically using a rhodamine-conjugated secondary antibody (Fig. 3). Nuclei were stained blue using DAPI. In positively transfected cells gfp-CRIP100 had a strong cytoplasmic expression. The majority of PR B protein was detected in cell nuclei, with some weak cytoplasmic staining in the untreated cells. Treatment with either R5020 or RU486, resulted in tight nuclear PR B staining, with very little PR detected in the cytoplasm of these cells. In contrast, gfp-CRIP100 remained cytoplasmic irrespective of hormone treatment. Furthermore, PR B localization was not affected by over-expression of gfp-CRIP100, and did not differ between transfected and untransfected cells.

Effect of CRIP100 on transcriptional activity of PR: The full length CRIP100 protein was not a ligand-dependent transcriptional activator of PR or GR although it did have weak transcriptional activation properties overall. When transfected into PR negative HeLa cells in increasing concentrations with a constant amount of PR B and a progestin-responsive luciferase reporter, reporter activity was weakly enhanced with increasing amounts of CRIP100 protein (Fig. 4). This was seen in the presence (hatched bars) or absence (plain bars) of the agonist R5020, suggesting that although CRIP100 increased the availability of PR to activate transcription on its reporter, it was not a true ligand dependent coactivator of PR. These data combined with cell localization results, suggested a role for CRIP100 during the initial steps of translation and folding of PR. This hypothesis was tested by a thorough analysis of CRIP100 interaction with PR and molecular chaperones known to be involved in PR folding.

Binding to PR: Immunoprecipitation was used to further study the binding of CRIP100 to both receptor forms A and B. Two variants of the human breast cancer cell line T47D were analyzed; one, YA, expressing exclusively the PRA isoform and the other, YB, expressing exclusively PRB. Antibodies were used to specifically immunoprecipitate PRA, PRB, or CRIP100 from cell lysates and the immunoprecipitated proteins were resolved by SDS-PAGE and analyzed by western blotting. As shown in Fig. 5, CRIP100 was detected in complexes with each PR species. When an antibody to CRIP100 (AbS1) was used for immunoprecipitation, co-precipitation of PR-A was clearly observed, but that for PR-B was barely detectable with this technique. Thus, both receptor species can be observed in complexes with CRIP100, although their abundance in these complexes may differ.

CRIP100 is incorporated during the assembly of PR chaperoning complexes in a cell-free system: Steroid receptor-chaperone complexes can be assembled in vitro using either rabbit reticulocyte lysate (25,27) or purified chaperone proteins (22,27). To further characterize CRIP100/PR interaction, we analyzed CRIP100 incorporation into newly reconstituted PR complexes using reticulocyte lysate, where CRIP100 was transcribed, translated and radiolabeled with ^{35}S-methionine. Human PRA and B were isolated from T47D YA and YB cytosols, respectively, by adsorption to antibody resin under high salt conditions that remove associated chaperones. The preparations were then incubated at 30°C in the presence of reticulocyte lysate containing ^{35}S-labeled CRIP100. The incorporation of CRIP100 into the reassembled PR complexes was assessed by autoradiography (Fig. 6A). The amounts of PR were assessed by western blotting (Fig. 6B). There was a low level of nonspecific binding of CRIP100 to the PR6 and AB52 antibodies (lanes 2, 4, 7). Nonetheless, CRIP100 was clearly incorporated into human PRA (lane 3) and PRB (lane 1) complexes. CRIP100 was also readily incorporated into avian

PRA/B complexes reconstituted in vitro (lane 6). These results further suggest that CRIP100 may be involved in the chaperone-dependent process of PR folding and maturation.

CRIP100 is incorporated into PR chaperoning complexes using a purified system: To gain more insight into CRIP100 recruitment in PR complexes, we used the PR from the chicken oviduct to test whether a purified chaperone system (consisting of hsp90, hsp70, Hop, hsp40 and p23) (22) was sufficient to incorporate CRIP100 into PR complexes and whether CRIP100 altered PR complexes. Chicken PR was used because methods for its isolation and analysis in vitro are much more clearly defined compared to human PR. The results are shown in Fig. 6C. Classical PR complexes containing hsp90, hsp70, hsp40 and p23 are shown in lane 5. Including CRIP100 resulted in its incorporation into the complexes (lane 6). This was observed as an increase in intensity of the protein band running at about 100 kDa since CRIP100 and PR-B have the same mobility on SDS-PAGE. CRIP100 incorporation was consistently accompanied with a slight decrease of hsp90 and p23 and a slight increase of hsp70 levels suggesting that CRIP100 may have some influence on the dynamics of assembly of PR complexes. To gain further understanding of the mechanism by which CRIP100 enters the reconstituted PR complex, we examined the possible direct interaction of CRIP100 with PR.

CRIP100 interacts with PR directly: CRIP100 was identified as a PR binding protein and it contains four LXXLL motifs that in other systems are known to mediate interactions between nuclear receptors and co-activators (13,26). The results shown above could not distinguish CRIP100-PR binding from some indirect interactions of CRIP100 with other PR-associated proteins. The first evidence for direct interaction of CRIP100 with PR was obtained by immunoprecipitation of purified CRIP100 with PRA/B linked to PR22 antibody resin (not

shown). To test whether CRIP100 interacts with both isoforms PR-A and PR-B, we first isolated PR-B from chick oviduct cytosol using an antibody (PR6) specific for PR-B (see Fig. 7A, lane 2). The remaining PR, now enriched in PRA, was then isolated using a more general PR antibody (PR22) (lane 4). CRIP100 readily bound to both PR preparations indicating its ability to bind directly to the different isoforms (lanes 3 and 5).

Additional experiments on the nature of CRIP100-PR binding found the binding to be very temperature-dependent with optimal binding at 37C (Fig. 7B). The interaction was relatively inefficient at temperatures below 30C, indicating that the binding may be accompanied by significant conformational changes in either or both CRIP100 and PR. Time course experiments at 37C, however, showed a relatively rapid interaction (Fig 7C). Approximately 50% of the binding occurred in the first five minutes of incubation.

Binding to hsp90: The full length CRIP100 clone contains three putative TPR domains. TPR domains are involved in protein-protein interactions and have been described in a number of proteins that interact with the PR chaperone hsp90 (24,28,29). Therefore, mammalian 2-hybrid assays were used to investigate a possible interaction between CRIP100 and hsp90, and to determine whether this influenced the dynamics of the PR-chaperone complex. In this assay hsp90 was expressed as a fusion with the gal4 DNA binding domain and CRIP100 was linked to the activation domain of VP-16. Interaction between the fusion proteins in a transient transfection assay resulted in activation of a gal4-luciferase reporter. When the hsp90 and CRIP100 constructs were cotransfected into HeLa cells along with the reporter, an interaction was consistently observed between the two proteins. When the hsp90 and CRIP100 constructs were co-transfected into HeLa cells along with the reporter, an interaction was consistently

observed between the two proteins and this was not changed when cells also contained PR (Fig. 8A, samples 1 and 2). This experiment also confirms an interaction between CRIP100 and PR (sample 3) and PR and hsp90 (sample 4). The addition of exogenous CRIP100 may slightly enhance the interaction between hsp90 and PR (sample 5). [In a similar experiment (Fig. 8B), the binding of hsp90 to CRIP100 was not altered by the agonist R5020 or the antagonist RU486 (group 1). However, this interaction was lost when cells also contained PR and were treated with RU486 (group 2). This suggests that the PR can sequester Gal4-hsp90 or VP16-CRIP100, but only in the presence of RU486. The binding between Gal4-PR and VP16-CRIP100 was lost by treatment with R5020 which is consistent with the possibility that CRIP100 only interacts with PR when in the chaperone complex in the absence of hormone (group 3). RU486 also causes a loss of this interaction. This suggests that the RU486 effect in group 2 is caused by an enhanced interaction of PR with Gal4-hsp90, not with VP16-CRIP100. Finally, the interaction between Gal4-hsp90 and VP16-PR was disrupted by R5020, but strongly enhanced by RU486. This is consistent with the view that agonists alter the PR to a form that no longer binds to hsp90 whereas the antagonist RU486 doesn't do this and appears to enhance chaperone interactions.]

The association of CRIP100 with hsp90 complexes was confirmed in co-precipitation assays using an antibody to hsp90 (H9010) (Fig. 8B) to isolate complexes or endogenous proteins from T47D cell cytosols. A blot using specific antibody for CRIP100 clearly indicated the presence of CRIP100 in complex with hsp90. Taken together, these results further expanded the protein multicomplexes of PRA, PRB and hsp90 to contain the CRIP100. Thus, it was necessary to define direct versus indirect interactions among these proteins.

To test the direct binding of CRIP100 to hsp90 in vitro we used antibody pull-down experiments with purified proteins (hsp90, CRIP100 and GST-CRIP100). As shown in Fig. 9A, GST-

CRIP100 adsorbed to glutathione-Sepharose was able to pull down hsp90 (lane 2), but this interaction was inefficient. The reciprocal experiment, however, using hsp90 bound to antibody resin, and CRIP100 without GST showed a much stronger level of binding (Fig. 5A, lane 3). The conformation and activity of hsp90 can be influenced by the binding of ATP or ADP, or by the hsp90 inhibitors geldanamycin and radicicol (30-32). When these agents were tested, they had little or no effect on the binding of CRIP100 (Fig. 9B).

Seeking a better understanding of CRIP100/hsp90 interaction, we analyzed the affinity of this interaction. A set amount of hsp90 was incubated with a range of CRIP100 concentrations and complexes were adsorbed to antibody resin to hsp90 and analyzed by SDS-PAGE. The binding of CRIP100 to hsp90 was saturable and the results fit a classical hyperbolic plot indicating a simple model of protein/protein interaction (Fig. 9C). A linear Scatchard plot (Fig. 9D) confirmed this interpretation and showed that CRIP100 bound hsp90 with high affinity (K_d = 43 nM). Measurements by densitometry indicated the CRIP100:hsp90 ratio at saturation to be about 1:1 by mass or two monomers of CRIP100 per dimer of hsp90.

CRIP100 has distinct binding sites for PR and hsp90. As shown in Fig. 9A, CRIP100 bound more efficiently after cleavage of GST. This observation suggested that CRIP100's TPR motifs near the N-terminus, might be important in binding hsp90. To directly test the importance of CRIP100's TPR domains in binding to hsp90, we tested proteins with point mutations of amino acids in TPR1 or TPR2. TPR repeats are degenerate 34 amino acid sequences with no position characterized by an invariant residue. However, certain amino acids are commonly observed in particular positions (33,34). Alignment of TPR sequences (Fig. 10A) showed that lysine 13 and alanine 20, located in helix loops A and B respectively, are conserved not only within CRIP100

TPR-motifs but also in most of the TPR motifs of Hop, FKBP52, FKBP51, cyp40 and PP5. Therefore, these two residues were mutated to glutamic and aspartic acid in the TPR1 and TPR2 repeats of CRIP100. Both mutations of TPR1 and TPR2 abrogated CRIP100-hsp90 interaction (Fig. 10B), suggesting that the two motifs are essential for hsp90 binding. Importantly, the three-dimensional structures of both mutants appeared to be stable and similar to CRIP100 wild type because they 1) co-migrated with CRIP100 wild type in size exclusion chromatography analysis with no signs of aggregation (not shown), and 2) retained binding to PR in a similar manner to the wild type (Fig. 10C).

The original 1kb clone that relieved growth suppression when cotransformed into yeast with the PR bait contained only the third and fourth LXXLL motifs (Fig. 1C) and none of the TPR domains. To determine whether one or both of these C-terminal LXXLL motifs were involved in the interaction between CRIP100 and PR, mutant constructs were prepared for use in a yeast two-hybrid assay. The constructs consisted of the initial 1kb C-terminal clone, with a leucine to alanine mutation at position four of LXXLL motif 3 (NRm3) or 4 (NRm4) as indicated in Figure 1C. As well as assessing the ability of the clones to relieve growth suppression when cotransformed into yeast with the PR bait, a colorimetric assay was performed to determine β-galactosidase activity from a cotransformed Gal4 reporter. As shown in Fig. 1A, the wild-type CRIP100 C-terminal clone relieved growth suppression when cotransformed with the PR bait into L40 yeast cells and plated onto selective media containing RU486 (Fig.11C). No growth was observed in the absence of RU486. Furthermore, the colorimetric assay confirmed these results. The NRm3 mutant in which LXXLL motif 3 had been disrupted was not able to rescue growth when cotransformed into cells with the PR bait. In contrast, the LXXLL motif 4 mutant NRm4 was as effective as the wild-type C-terminal CRIP100 clone in rescuing cell growth.

Further analysis of the importance of the four NR motifs in PR binding by the full length protein was performed in vitro by double point mutations of both leucine 1 and 2 in each of the four LXXLL sequences individually. The two mutations changed the leucine residues to serine. Surprisingly, the four generated mutants seem to interact similarly to the wild type with PR (Fig. 11A) and with hsp90 (Fig. 11B), indicating that the four motifs might be complementary or are not required for the *in vitro* binding and suggest a more complex mechanism of interaction in vivo.

CRIP100 and Hop have distinct binding sites on hsp90. To further understand the nature of CRIP100/hsp90 interaction, we used an indirect competition test with Hop. Hop was chosen for several reasons: 1) It was shown to compete with other TPR motifs containing proteins, such as immunophilins and PP5, in hsp90 binding tests (35,36); 2) It does not directly interact with CRIP100 in immunoprecipitation experiments using a Hop specific antibody (not shown); 3) Biochemical studies have shown that Hop (or yeast Sti1) is a dimer in solution suggesting that binding of Hop to hsp90 should simultaneously occupy the two independent TPR-domain-binding sites of hsp90 dimer (37); 4) Hop and CRIP100 have comparable affinities in binding hsp90 (38) (Fig. 5D).

When hsp90 was saturated with CRIP100 and increasing amounts of Hop were added, Hop was incorporated in the hsp90 complex without affecting the amount of CRIP100 bound (Fig. 12B). Reverse experiments, where hsp90 was first saturated with Hop showed similar results (not shown). These unexpected findings strongly suggest that hsp90 binds simultaneously both TPR proteins in a noncompetitive manner. Thus, hsp90 appears able to bind both CRIP100 and Hop in a ternary complex. This interpretation is further confirmed by the fact that the hsp90-Hop

complex, immunoprecipitated using Hop specific antibody, also immunoprecipitated CRIP100 (Fig. 12C, lane 3). Densitometry analysis of CRIP100, hsp90 and Hop in this complex showed mass ratios of about 1:1:1 suggesting two monomers of CRIP100 and one dimer of Hop bind per hsp90 dimer.

CRIP100's binding site on hsp90 is located in the N-terminal domain of hsp90. Hop interaction with hsp90 involves primarily a TPR recognition motif (MEEVD) in the C-terminus of hsp90. Since CRIP100's TPR motifs were essential for hsp90 binding, and Hop did not compete in this interaction, it seemed likely that hsp90 contains a second TPR binding site. To test this hypothesis we used several C-terminal deletion fragments of hsp90 to map the binding site for CRIP100. Pull-down experiments of CRIP100 with these fragments demonstrated that hsp90's N-terminal domain 1-332 was sufficient for the binding of CRIP100 (Fig. 13). [However, this fragment does not bind the TPR mutants of CRIP100 (not shown)]. These findings clearly establish the existence of a second TPR recognition site within the first 1-332 residues of hsp90 and provide a molecular basis for a model where hsp90 binds CRIP100 by the N-terminal and Hop via the C-terminal TPR recognition motif MEEVD. Taken together, these data suggest the existence of noncompetitive TPR-co-factors interacting with hsp90 with the potential for interesting regulatory effects on hsp90 function.

Discussion

Association of nascent PR with the hsp90 chaperone pathway is an essential first event in the molecular action of PR. Hsp90 binds directly to the hormone-binding domain of PR and abrogation of this binding inhibits the transcriptional activity of PR. In turn, hsp90 associates with numerous other partner proteins, which together form the multiprotein chaperone complex responsible for PR folding and stabilization. The roles played by all the members of the chaperone complex are only partially characterized at this point.

We report here the finding of a novel protein CRIP100 which binds directly to the PR and to hsp90. Analysis of CRIP100's sequence revealed an interesting combination of structural motifs that make it a potentially important player in the steroid receptor chaperoning pathway. Indeed, CRIP100 contains four LXXLL sequences that are known to be important in the interaction of nuclear receptors with co-activators (13,26). It also contains three TPR motifs suggesting that CRIP100 is a potential hsp90-interacting protein (28,35,37). In this study, we showed that CRIP100 is part of PR and hsp90 complexes immuno-isolated from cell lysates. Furthermore, we demonstrated and partially characterized its direct interactions *in vitro* with hsp90 and both isoforms of PR. We also established that CRIP100 can be incorporated along with other molecular chaperones during PR complex reassembly in cell-free systems.

The precise region and residues of CRIP100 that interact with PR are yet to be defined. Heery et al. proposed that the LXXLL motif is a signature sequence that facilitates the interaction of different proteins with nuclear receptor (26). Our mutational studies of the LXXLL sequences however, clearly show that no single sequence is essential for CRIP100/PR binding to occur *in vitro*. However, in our initial studies on CRIP100, we found that a fragment that contained the

third and fourth LXXLL motifs was able to bind PR in a yeast two-hybrid system. Mutation analysis showed that motif three was essential for this interaction, but not motif four. One possible explanation for these results is that the mutation of motif three in the full-length protein can be compensated by motif one or two. More complete studies are underway to better define this interaction both *in vivo* and *in vitro*.

CRIP100 interacts with hsp90 through its TPR motifs as evidenced by the loss of binding caused by double mutations of residues in TPR1 and TPR2 motifs. These mutations targeted lysine 13 and alanine 20 of each TPR motif because these residues are conserved not only in CRIP100's TPR motifs but also among TPR-motifs of other TPR co-chaperones involved in hsp90 binding (21,28,33,36). In addition, based on previous crystal structures of hsp90's TPR co-chaperones, Lys13 and Ala20 would be respectively located in the antiparallel alpha helices A and B that constitute the backbone structure of TPR motifs. One model of interaction with TPR motifs postulates that a right-handed super-helical structure generated by the folding of tandem TPR motifs forms a binding groove that accommodates target proteins (28,33). Hence, changing Lys13 and Ala20 residues to acidic amino acids would have caused electrostatic changes in the two TPR motifs which may result in perturbations at one or several levels: 1) locally in the individual motif, 2) in the overall structure of the TPR domain, or 3) in parts of the molecule outside of TPR domain. Our data, however, suggest that these changes cannot be of a major scale because three-dimensional structures of the mutants, at least as assessed by size exclusion chromatography, are identical to wild type (not shown) and their PR binding capabilities are entirely preserved (Fig. 6C). Thus, we hypothesize that the alpha helices of CRIP100 TPR1 and TPR2 are the primary components of the hsp90 binding site. Binding may be facilitated by additional interactions outside this region as has been indicated for binding to hsp90 (39).

Since the TPR domains of CRIP100 are involved in hsp90 binding, it seemed likely that the C-terminus of hsp90 would be the site of this interaction, as has been shown for Hop and the immunophilins (28,40,41). Surprisingly, however, the TPR recognition motif MEEVED in the C-terminus of hsp90 is not required for CRIP100 interaction as demonstrated by the fact that Hop and CRIP100 bind to hsp90 in a noncompetitive manner (Fig. 8) and, more directly, by the ability of the N-terminal fragment 1-332 of hsp90 to pull down CRIP100 in co-immunoprecipitation experiments (Fig. 9). These findings strongly support the existence of distinct binding sites for CRIP100 and Hop on hsp90 and suggest, for the first time, the presence of another TPR recognition site in the 1-332 N-terminus of hsp90.

Hsp90's fragment 1-332 is composed of an ATP binding domain (1-210), the highly charged region (206-280) and ~ 50 residues downstream of the charge region (Fig. 10). Interestingly, the N-terminal domain (1-210) has been shown to interact with and "chaperone" denatured proteins and hydrophobic peptides *in vitro*, which has been interpreted as an indication that this region binds hsp90 client proteins. This "chaperoning activity" is ATP and geldanamycin sensitive, but is not altered by ADP (42,43). This region is also involved in the binding of the co-chaperone p23 (44). The binding of p23 requires that hsp90 exist as a dimer with bound ATP. CRIP100 interaction adds yet another binding capacity for the N-terminal region of hsp90 and it is somewhat surprising that this interaction is not markedly influenced by ATP or geldanamycin. Preliminary studies show that the binding of CRIP100 to hsp90 does not block the binding of either ATP or p23, however, additional studies are needed to evaluate more subtle interrelationships among these interactions.

Taken together, our data raise intriguing parallels between CRIP100-hsp90-Hop interactions and hip-hsp70-Hop binding. Mutagenesis studies showed indeed, that TPR repeats are required for hip binding to hsp70 (45); nevertheless, the co-chaperone interacts exclusively with a sequence yet to be identified in the amino-terminal ATPase domain of hsp70 (45,46). Hop binding, on the other hand, requires the EEVD sequence in the C-terminus of the chaperone. The function of Hip is still unclear, but it appears to stabilize the ADP-bound state of hsp70 (47).

In the chaperoning process for PR, Hop binds to both hsp70 and hsp90 to link their chaperoning functions (48). In this intermediate complex, the PR lacks hormone-binding activity. This activity is acquired in the transition to a mature complex where ATP, p23 and immunophilins are bound to hsp90 and there is a reduction in the presence of hsp70 and Hop (1). It is believed that important conformational changes in both hsp90 and PR occur at this step. The interactions of CRIP100 with both PR and hsp90 are very temperature-dependent suggesting that they are accompanied by marked conformational changes. It is still unclear whether CRIP100 enters PR-chaperone complexes at the intermediate step or at the mature complex. When present in PR complexes, CRIP100 causes a slight reduction in the binding of hsp90 and p23, perhaps because of its influence on the conformational state of PR or hsp90. Such influences could also alter hormone-binding activity. CRIP100 was initially identified as a protein that was selective for PR bound with the antagonist RU38486. It is tempting to speculate that this selectivity arose through chaperone-mediated changes in the hormone binding specificity of the PR. Studies are in progress to investigate this and to identify the biological functions of CRIP100.

Figure Legends

Fig. 1: Characterization of novel PR-interacting protein CRIP100.

A – The interaction between CRIP100 and the hinge-HBD region of PR was confirmed in the yeast 2-hybrid assay. The L40 yeast strain was transformed with the plasmid constructs: 1 – CRIP100 + pBTM116:hHBD-PR, 2 – CRIP100 + pBTM116:lamin, 3 – pGAD112, 4 – CRIP100 alone, 5 – pBTM116:hHBD-PR alone, or 6 – positive control construct. The transformed cells were plated on synthetic dextrose agar dropout plates (SD-LEU-TPR-HIS) containing 10 mM RU486 or vehicle, as indicated, and growth was monitored for 3 to 5 days at 30C.

B – Interaction between gst-CRIP100 and PR A, PR B and GR: HeLa cell lysates containing transfected PR A, PR B or GR, were incubated 1h at 4C with gst-CRIP100 bound Sepharose or gst-alone Sepharose in the presence of 10nM R5020, 100 nM RU486 or 10 nM dexamethasone, as indicated. Protein-bound Sepharose samples were pelleted and washed as indicated in materials and methods. Samples were fractionated on 7.5% SDS-PAGE and PR and GR were visualized by immunoblotting.

C – Mutational analysis of NR box-like motifs in the C-terminal CRIP100 clone. A schematic of the CRIP100 protein is shown. The locations of three TPR domains and four putative NR box motifs are indicated, as well as the start of the original CRIP100 clone fragment identified in the PRhHBD yeast two-hybrid screen. The sequence substitutions of site-directed NR box mutants, NRm3 and and NRm4 are indicated.

Fig. 2: Detection of CRIP100 mRNA transcript and protein.

A – A multiple human tissue RNA blot (Clontech) was probed with a ^{32}P-labeled 1kb C-terminal fragment of the CRIP100 cDNA, following the manufacturer's instructions. Relative spot intensities representing CRIP100 transcript levels in each tissue were estimated by densitometry.

Inset – CRIP100 transcripts were visualized in 30 mg total RNA isolated from HeLa cervical cancer and T47Dco breast cancer cell lines by northern blotting. Transcript size was estimated using a commercial RNA ladder, and the positions of 18S and 28S rRNA subunits are indicated. **B** – CRIP100 protein detected by immunoblot in rodent tissues and human cell lines. Cytosols from mouse tissues: 1. Lung, 2. Heart, 3. Kidney, 4. Liver, 5. Spleen, 6. Muscle, 7. Tongue, 8. Brain, 9. Testis, 10. Uterus, 11. Rat brain cytosol, 12. IP from Rat brain cytosol, 13. Human Ovarian cancer cell line OVCAR-8 cytosol and 14. Immunoprecipitated protein, 15. Human Ovarian cancer cell line MDAH2774 cytosol and 16. Immunoprecipitated protein, 17. Human Ovarian cancer cell line PA1 cytosol and 18. Immunoprecipitated protein.

Fig. 3: Effect of CRIP100 on PR transcription.

HeLa cells were transfected with 10 ng hPR1, 1 mg PRE_2-$TATA_{dk}$-LUC and 250 ng pCH110, in the presence of increasing quantities of CRIP100 as indicated. Luciferase and β-galactosidase activities were estimated in harvested cell lysates after 16-20h treatment of the cells with 10 nM R5020 (striped bars) or vehicle (open bars). Reporter activity is shown corrected for β-galactosidase activity.

Fig. 4: Cellular localization of CRIP100 protein.

The pEGFP-C1-93 construct, containing the CRIP100 cDNA fused C-terminally to green fluorescent protein, was transfected into PR+ T47D-YB growing on coverslips. Two days after transfection cells were tested for 1h with 10 nM R5020, 100 nM RU486 or vehicle, then fixed and stained for PR expression, as described in materials and methods. Nuclei were visualized using DAPI.

Fig. 5: CRIP100 is expressed by T47D cells and is a component of human PR and chaperone complexes.

A. Endogenous CRIP100, PRA and PRB were immunoprecipitated from T47D YA or YB cytosols using the monoclonal antibodies, AbS1 (CRIP100) and AB52 (PR). Mouse IgG (M.IgG) was used to evaluate the non-specific background of immunoprecipitation. Bound proteins were resolved by SDS-PAGE and transferred onto PVDF membrane. The membrane was first incubated with AbS1 to detect CRIP100 and then incubated with AB52 to detect human PRA or PRB. **B**. Immunoprecipitations of endogenous CRIP100 and hsp90 were performed as in A using AbS1 and H9010 monoclonal antibodies respectively and blotted with AbS1 antibody to detect CRIP100.

Fig. 6: CRIP100 is incorporated into PR complexes during reassembly in a cell-free system. **A** and **B**. 35S methionine-labeled CRIP100 was generated by in vitro translation. (RL*) and used to test CRIP100 incorporation into PR from T47D YA or YB cells and from chicken oviduct cytosols using monoclonal antibodies PR6, AB52 and PR22 respectively. Lanes 2, 4 and 7 show the backgrounds (without PR). Bound proteins were resolved by SDS-PAGE and transferred to PVDF membrane. The radioactive CRIP100 (Panel A) was detected using a phosphoimager (). The radioactivity given by 1 μl of translation reaction is shown in lane 5. The appearance of human or chicken PR was detected by western blotting (panel B). **C**. Avian PRA/B was isolated from oviduct cytosol using antibody PR22 bound to protein A-Sepharose and stripped of associated proteins (lane 4). PR complexes were then reconstituted using purified proteins (hsp90, hsp70, Hop, hsp40 and p23) in the absence (lane 5) or presence (lane 6) of CRIP100. Lanes 2 and 3 show the level of interaction of the five proteins or CRIP100 with antibody resin0.

The mobility of each protein is as indicated on the right as well as antibody heavy (HC) and light (LC) chains. Molecular weight markers in kDa are indicated on the left.

Fig. 7: CRIP100 interacts directly with PR.

A. Avian oviduct cytosol was incubated first with PR6-protein A-Sepharose resin to isolate PRB (lane 2). Then cytosol "depleted" of PRB was incubated with PR22 resin to isolate PRA (lane 4). Each PR subtype was tested for binding CRIP100 (lanes 3 and 5). **B**. Stripped PR was incubated with 20 μg of CRIP100 at the indicated temperatures for 15 min. **C**. Stripped PRA/B was incubated at 37C with 20 μg of CRIP100 for the indicated time. For control, CRIP100 was incubated with PR22 resin without receptor at 37C for 40 min.

Fig. 8: Interaction between CRIP100, hsp90 and PR.

A – Constructs containing CRIP100, PR B and hsp90 linked to the Gal4DNA binding domain and VP16 activation domain were cotransfected into HeLa cells as indicated, and harvested two days later. Where indicated the PR B and CRIP100 constitutive expression vectors were included in the transfection. Protein-protein interactions were estimated as luciferase activity arising from a cotransfected Gal4 response element reporter, and are shown corrected for β-galactosidase activity. The Gal4-hsp90 and pVP16 CRIP100 constructs were cotransfected with empty VP16 and Gal4DBD controls, respectively (right two bars). Error bars represent the standard deviations of triplicate determinations.

B –Endogenous CRIP100, and hsp90 were immunoprecipitated from T47D YA or YB cytosols using respectively the monoclonal antibodies AbS1 and H9010. Bound proteins were resolved by SDS-PAGE and blotted with AbS1 antibody to detect CRIP100.

Fig. 9: Analysis of CRIP100 interaction with hsp90.

A Analysis of direct interaction between hsp90 and CRIP100 was carried out by pull down experiments with glutathione resin (lane 2) or immunoprecipitation by H9010 antibody after cleavage of GST (lane 3) using purified proteins. Lane 1 shows background of CRIP100 bound to the glutathione resin, and lane 4, to resin H9010 Protein A without hsp90. Proteins were resolved by SDS-PAGE and stained with Coomassie blue. **B**. Purified CRIP100 was incubated with H9010 bound hsp90 in the presence of no nucleotide, 5 mM ATP, 5 mM ADP, 50 μM geldanamycin (GA) or 50 μM radicicol (rad). In lane (C), H9010 resin lacking hsp90 was incubated with 10 μg CRIP100 with no ligand. CRIP100 and hsp90 positions are shown. All incubations were at (30C) for 40 min. **C**. Increasing amounts of CRIP100 (1-30 μg) in duplicate were added to samples of immobilized hsp90 (2 μg) and incubated for 40 min at (30C). Coomassie stained bands were quantified by densitometry. The plot of arbitrary units (AU) of bound CRIP100 is shown and represents the mean values for each concentration. All experiments were repeated at least two times. **D**. Scatchard analysis of panel **C** values.

Fig. 10: TPR motifs of CRIP100 are essential for hsp90 binding.

A. Comparison of TPR motifs of CRIP100, Hop, FKBP52, FKBP51, cyp40 and PP5. Mutated amino acids are shaded. Helices A and B of each TPR repeat motif are indicated according to ().

B. Co-immunoprecipitation of 2 μg of CRIP100 wild type (lane 3), TPR1 (lane 5) and TPR2 (lane 7) mutants with 5 μg of hsp90 bound to H9010 antibody. Lanes 2, 4, 6 represent CRIP100 resin controls. **C.** Co-immunoprecipitation of CRIP100 wild type (lane 3), TPR1 (lane 5) and TPR2 (lane 7) mutants with avian PRA/B using PR22 antibody. Lanes 2, 4, 6 show the background without PR.

Fig. 11: The binding of CRIP100 NR mutants to PR. **A**. Double point mutation in each NR sequence of CRIP100 were prepared. Purified CRIP100 wild type and mutants NR1, NR2, NR3 and NR4 were incubated with stripped avian PRA/B bound to antibody (PR22) resin. Nonspecific bindings were assessed by proteins incubated with antibody resin without PRA/B. Samples were washed and bound proteins resolved by SDS-PAGE and stained with Coomassie blue. **B.** Wild type and NR mutants were tested for hsp90 binding using hsp90 monoclonal antibody H9010 and following the same procedure as in A. **C**. The performance of two mutants, NRM3 and NRM4 in growth and colorimetric yeast two-hybrid assys.

Fig. 12: CRIP100 and Hop interact with different parts of hsp90.

A. Purified CRIP100 was incubated with Hop antibody resin in the absence (lane 1) or presence (lane 2) of prebound Hop. The complexes were washed, resolved by SDS-PAGE and stained with Coomassie blue. **B**. Hsp90 (-μg) was bound to antibody resin and then saturated with CRIP100 (-μg). Excess CRIP100 was removed and samples were incubated with increasing amounts (0-40 μg) of Hop. Complexes were isolated and analyzed by SDS-PAGE. Gels were stained with Coomassie blue and scanned. Densitometry values for CRIP100 and Hop are plotted against amount (μg) of Hop added in the reaction mixture. **C**. Hop and hsp90 were incubated with the Hop antibody resin. Excess protein was removed by centrifugation and the resin complex was incubated with 10 μg of CRIP100 and 5 mM ADP for 30 min. at 37C. The complex was isolated and resolved by SDS-PAGE (lane 3). Background binding of hsp90 and CRIP100 to antibody resin without Hop are shown in lane 2. $1/10^{th}$ of protein loads are shown in lanes 4-6.

Fig. 13: The CRIP100 binding site is located within N-terminal domain of hsp90.

N-terminal-tagged GST-hsp90 and different C-terminal deletion fragments along with hsp90 without tag were used to pull down CRIP100 using hsp90 BF4 antibody resin. Samples were washed and bound proteins analyzed by SDS-PAGE. Background of CRIP100 bound to antibody resin alone is shown in lane 9.

References

1. **Pratt, W. B. and D. O. Toft.** 2003. Regulation of signaling protein function and trafficking by the hsp90/hsp70-based chaperone machinery. Exp. Biol. Med. **228:**111-133.

2. **Freeman, B.C. and K.R. Yamamoto**. 2002. Science **296:**2232-2235.

3. **Elbi, C., D.A. Walker, G. Romero, W.P. Sullivan, D.O. Toft, H.L. Hager, and D.B. DeFranco.** Molecular chaperones function as steroid receptor nuclear mobility factors. Proc. Natl. Acad. Sci., USA (in press).

4. **Shibata, H., T.E. Spencer, S.A. Onate, G. Jenster, S.Y. Tsai, M.J. Tsai, and O.M. BW.** 1997. Role of co-activators and co-repressors in the mechanism of steroid/thyroid receptor action. Recent Prog. Horm. Res. **52:**141-164.

5. **Glass, C.K., D.W. Rose, and M.G. Rosenfeld.** 1997. Nuclear receptor coactivators. Current Opinion Cell Biol. **9:**222-232.

6. **Horwitz, K.B., T.A. Jackson, D.L. Bain, J.K. Richer, G.S. Takimoto, and L. Tung.** 1996. Nuclear receptor coactivators and corepressors. Mol. Endocrinol. **10:**1167-1177.

7. **Tsai, M.-J. and B.W. O'Malley.** 1994. Molecular mechanisms of action of steroid/thyroid receptor superfamily members. Ann. Rev. Biochem. **63:**451-486.

8. **McKenna, N.J. and B.W. O'Malley.** 2002. Combinatorial control of gene expression by nuclear receptors and coregulators. Cell **108:**465-474.

9. **Young, J. C., I. Moarefi, and F. U. Hartl.** 2001. Hsp90: a specialized but essential protein-folding tool. J. Cell Biol. **154:**267-273.

10. **Richter, K. and J. Buchner.** 2001. Hsp90: Chaperoning signal transduction. J. Cell. Phys. **188:**281-290.

11. **Hernández, M. P., A. Chadli, and D. O. Toft.** 2002. HSP40 binding is the first step in the HSP90 chaperoning pathway for the progesterone receptor. J. Biol. Chem. **277:**11873-11881.

12. **Smith, D. F., L. Whitesell, S. C. Nair, S. Chen, V. Prapapanich, and R. A. Rimerman.** 1995. Progesterone receptor structure and function altered by geldanamycin, and hsp90-binding agent. Mol. Cell. Biol. **15:**6804-6812.

13. **Collingwood, T. N., F. D. Urnov, and A. P. Wolffe.** 1999. Nuclear receptors: coactivators, corepressors and chromatin remodeling in the control of transcription. J. Mol. Endo. **23:**255-275.

14. **King, F. W., A. Wasrzynow, J. Höhfeld, and M. Zylicz.** 2001. Co-chaperones Bag-1, Hop and Hsp40 regulate Hsc70 and Hsp90 interactions with wild-type or mutant p53. EMBO J. **20:**6297-6305.

15. **Panaretou, B., G. Siligardi, P. Meyer, A. Maloney, J. K. Sullivan, S. Singh, S. H. Millson, P. A. Clarke, S. Naaby-Hansen, R. Stein, R. Cramer, M. Mollapour, P. Workman, P. W. Piper, L. H. Pearl, and C. Prodromou.** 2002. Activation of the ATPase activity of Hsp90 by the stress-regulated cochaperone Aha1. Mol. Cell **10:**1307-1318.

16. **Lange, C. A., J. K. Richer, and K. B. Horwitz.** 1999. Hypothesis: Progesterone primes breast cancer cells for cross-talk with proliferative or antiproliferative signals. Mol. Endo. **13:**829-836.

17. **Levin, E. R.** Bidirectional signaling between the estrogen receptor and the epidermal growth factor receptor. Mol. Endo. **17:**309-317.

18. **Jackson, T.A., J.K. Richer, D.L. Bain, G.S. Takimoto, L. Tung, and K.B. Horwitz.** 1997. The partial agonist activity of antagonist-occupied steroid receptors is controlled by a novel hinge domain-binding coactivator L7/SPA and the corepressors N-CoR or SMRT. Mol. Endocrinol. **11:**693-705.

19. **Horwitz, K.B. and G.R. Freidenberg.** 1985. Growth inhibition and increase of insulin receptors in antiestrogen-resistent T47DCO human breast cancer cells by progestins: Implications for endocrine therapies. Cancer Res. **45:**167-173.

20. **Sartorius, C.A., S.D. Groshong, L.A. Miller, R.L. Powell, L. Tung, G.S. Takimoto, and K.B. Horwitz.** 1994. New T47D breast cancer cell lines for the independent study of progesterone B- and A-receptors: Only antiprogestin-occupied B-receptors are switched to transcriptional agonists by cAMP. Cancer Res. **54:**3868-3877.

21. **Sullivan, W. P., B. Stensgard, G. Caucutt, B. Bartha, N. McMahon, E. S. Alnemri, G. Litwack, and D. Toft.** 1997. Nucleotides and two functional states of hsp90. J. Biol. Chem. **272:**8007-8012.

22. **Kosano, H., B. Stensgard, M. C. Charlesworth, N. McMahon, and D. Toft.** 1998. The assembly of progesterone receptor-hsp90 complexes using purified proteins. J. Biol. Chem. **273:**32973-32979.

23. **Sullivan, W. P., T. G. Beito, J. Proper, C. J. Krco, and D. O. Toft.** 1986. Preparation of monoclonal antibodies to the avian progesterone receptor. Endocrinology **119:**1549-1557.

24. **Blatch, G.L. and M. Lassle**. 1999. The tetratricopeptide repeat: a structural motif mediating protein-protein interactions. BioEssays **21:**932-939.

25. **Smith, D. F., D. B. Schowalter, S. L. Kost, and D. O. Toft.** 1990. Reconstitution of progesterone receptor with heat shock proteins. Mol. Endo. **4:**1704-1711.

26. **Heery, D. M., E. Kalkhoven, S. Hoare, and M. G. Parker.** 1997. A signature motif in transcriptional co-activators mediates binding to nuclear receptors. Nature **387:**733-736.

27. **Dittmar, K. D., K. A. Hutchinson, J. K. Owens-Grillo, and W. B. Pratt.** 1996. Reconstitution of the steroid receptor-hsp90 heterocomplex assembly system of rabbit reticulocyte lysate. J. Biol. Chem. **271:**12833-12839.

28. **Scheufler, C., A. Brinker, G. Bourenkov, S. Pegoraro, L. Moroder, H. Bartunik, F. U. Hartl, and I. Moarefi.** 2000. Structure of TPR domain-peptide complexes: Critical elements in the assembly of the Hsp70-Hsp90 multichaperone machine. Cell **101:**199-210.

29. **Russell, L. C., S. R. Whitt, M.-S. Chen, and M. Chinkers.** 1999. Identification of conserved residues required for the binding of a tetracopeptide repeat domain to heat shock protein 90. J. Biol. Chem. **274:**20060-20063.

30. **Prodromou, C., B. Panaretou, S. Chohan, G. Siligardi, R. O'Brien, J. E. Ladbury, S. M. Roe, P. W. Piper, and L. H. Pearl.** 2000. The ATPase cycle of Hsp90 drives a molecular "clamp" via transient dimerization of the N-terminal domains. EMBO J. **19:**4383-4392.

31. **Chadli, A., I. Bouhouche, W. Sullivan, B. Stensgard, N. McMahon, M. G. Catelli, and D. O. Toft.** 2000. Dimerization and N-terminal domain proximity underlie the function of the molecular chaperone heat shock protein 90. Proc. Natl. Acad. Sci. **97:**12524-12529.

32. **Sullivan, W. P., B. A. L. Owen, and D. O. Toft.** 2002. The influence of ATP and p23 on the conformation of hsp90. J. Biol. Chem. **277:**45942-45948.

33. **Das, A. K., P. T. W. Cohen, and D. Barford.** 1998. The structure of the tetratricopeptide repeats of protein phosphatase 5: implications for TPR-mediated protein-protein interactions. EMBO J. **17:**1192-1199.

34. **Lapouge, K., S. J. M. Smith, P. A. Walker, S. J. Gamblin, S. J. Smerdon, and K. Rittinger.** 2000. Structure of the TPR domain of $p67^{phox}$ in complex with Rac·GTP. Mol. Cell **6:**899-907.

35. **Carrello, A., E. Ingley, R. F. Minchin, S. Tsai, and T. Ratajczak.** 1999. The common tetratricopeptide repeat acceptor site for steroid receptor-associated immunophilins and Hop is located in the dimerization domain of hsp90. J. Biol. Chem. **274:**2682-2689.

36. **Owens-Grillo, J. K., M. J. Czar, K. A. Hutchison, K. Hoffmann, G. H. Perdew, and W. B. Pratt.** 1996. A model of protein targeting mediated by immunophilins and other proteins that bind to hsp90 via tetratricopeptide repeat domains. J. Biol. Chem. **271:**13468-13475.

37. **Prodromou, C., G. Siligardi, R. O'Brien, D. N. Woolfson, L. Regan, B. Panaretou, J. E. Ladbury, P. W. Piper, and L. H. Pearl.** 1999. Regulation of Hsp90 ATPase activity by tetratricopeptide repeat (TPR)-domain co-chaperones. EMBO J. **18:**754-762.

38. **Hernández, M. P., W. P. Sullivan, and D. O. Toft.** 2002. The assembly and intermolecular properties of the hsp70-Hop-hsp90 molecular chaperone complex. J. Biol. Chem. **277:**38294-38304.

39. **Cheung-Flynn, J., P.J. Roberts, D.L. Riggs, and D.F. Smith.** 2003. C-terminal sequences outside the tetracopeptide repeat domain of FKBP51 and FKBP52 cause differential binding to Hsp90. J. Biol. Chem. **278:**17388-17394.

40. **Chen, S., W.P. Sullivan, D.O. Toft, and D.F. Smith.** 1998. Differential interactions of p23 and the TPR-containing proteins Hop, Cyp40, FKBP52 and FKBP51 with Hsp90 mutants. Cell Stress and Chaperones **3:**118-129.

41. **Young, J.C., M.J. Obermann, and F.U. Hartl.** 1998. Specific binding of tetratricopeptide repeat proteins to the C-terminal 12-kDa domain of hsp90. J.Biol. Chem. **273:**18007-18010.

42. **Young, J. C., C. Schneider, and F. U. Hartl.** 1997. In vitro evidence that hsp90 contains two independent chaperone sites. FEBS Let. **418:**139-143.

43. **Scheibel, T., T. Weikl, and J. Buchner.** 1998. Two chaperone sites in Hsp90 differing in substrate specificity and ATP dependence. Proc. Natl. Acad. Sci. **95:**1495-1499.

44. **Chadli, A., I. Bouhouche, W. Sullivan, B. Stensgard, N. McMahon, M. G. Catelli, and D. O. Toft.** 2000. Dimerization and N-terminal domain proximity underlie the function of the molecular chaperone heat shock protein 90. Proc. Natl. Acad. Sci. **97:**12524-12529.

45. **Prapapanich, V., S. Chen, E. J. Toran, R. A. Rimerman, and D. F. Smith.** 1996. Mutational analysis of the hsp70-interacting protein Hip. Mol. Cell. Biol. **16:**6200-6207.

46. **Desmond, J., J. Lüders, and J. Höhfeld.** 1998. The carboxy-terminal domain of Hsc70 provides binding sites for a distinct set of chaperone cofactors. Mol. Cell. Biol. **18:**2023-2028.

47. **Hőhfeld, J., Y. Minami, and F.U. Hartl.** 1995. Hip, a novel cochaperone involved in the eukaryotic Hsc70/Hsp40 reaction cycle. Cell **83:**589-598.

48. **Chen, S. and D. F. Smith.** 1998. Hop as an adaptor in the heat shock protein 70 (Hsp70) and Hsp90 chaperone machinery. J. Biol. Chem. **273:**35194-35200.

Acknowledgments

We express our appreciation to Sara Felts for her critical reading of the manuscript and to Sherry Linander for the preparation of the manuscript. Also, we thank Bridget Stensgard for her technical assistance. This work was supported by NIH grant RO1 DK 59284.

Fig.1.

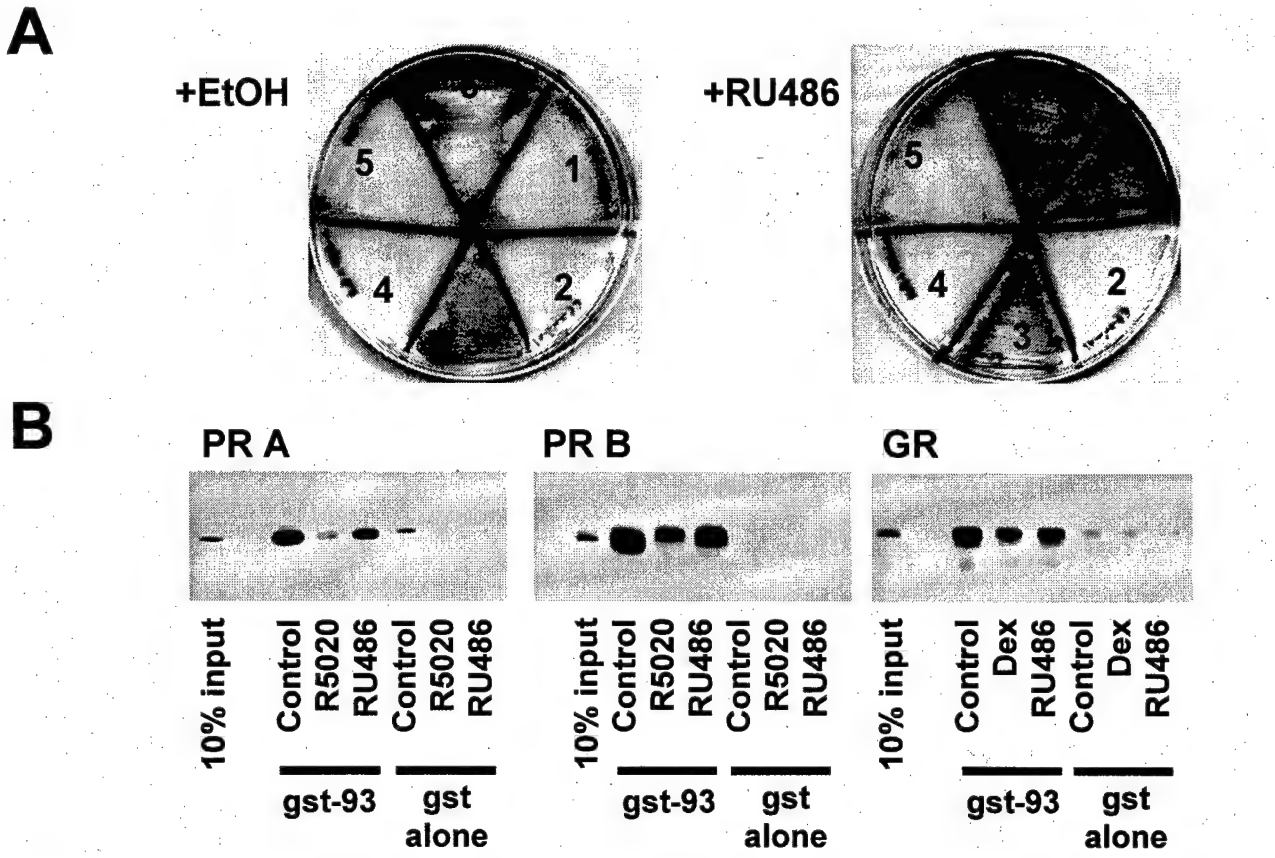

Target Construct	10^{-6}M RU486	Growth Assay	Color Assay
C-term wt	−	−	−
C-term wt	+	+	+
NRm3	+	−	−
NRm4	+	+	+
none	−	−	−
none	+	−	−

Fig.2.

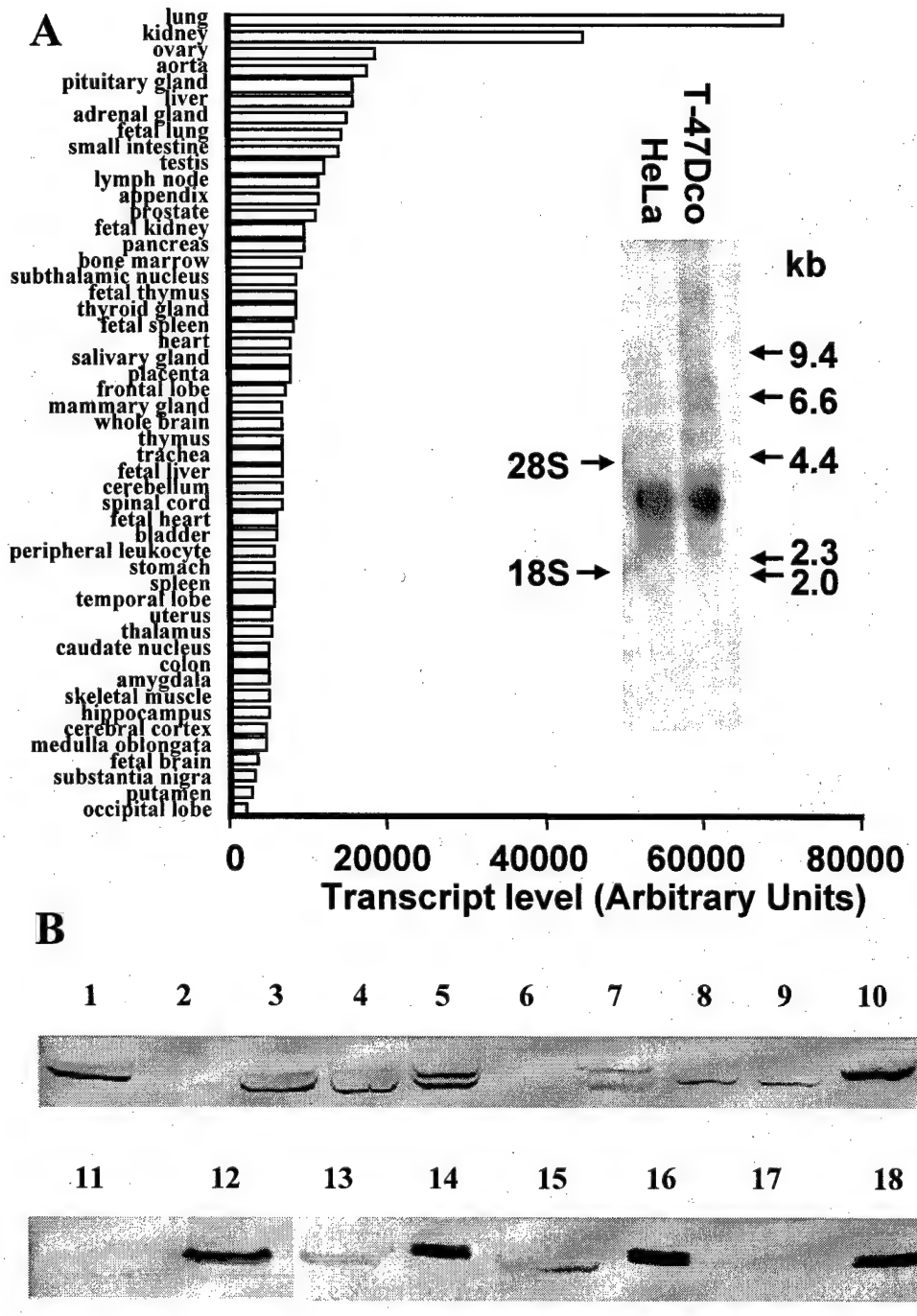
A
lung
kidney
ovary
aorta
pituitary gland
liver
adrenal gland
fetal lung
small intestine
testis
lymph node
appendix
prostate
fetal kidney
pancreas
bone marrow
subthalamic nucleus
fetal thymus
thyroid gland
fetal spleen
heart
salivary gland
placenta
frontal lobe
mammary gland
whole brain
thymus
trachea
fetal liver
cerebellum
spinal cord
fetal heart
bladder
peripheral leukocyte
stomach
spleen
temporal lobe
uterus
thalamus
caudate nucleus
colon
amygdala
skeletal muscle
hippocampus
cerebral cortex
medulla oblongata
fetal brain
substantia nigra
putamen
occipital lobe
0
20000
40000
60000
80000
Transcript level (Arbitrary Units)
HeLa
T-47Dco
kb
9.4
6.6
4.4
2.3
2.0
28S
18S
B
1
2
3
4
5
6
7
8
9
10
11
12
13
14
15
16
17
18

Fig.3.

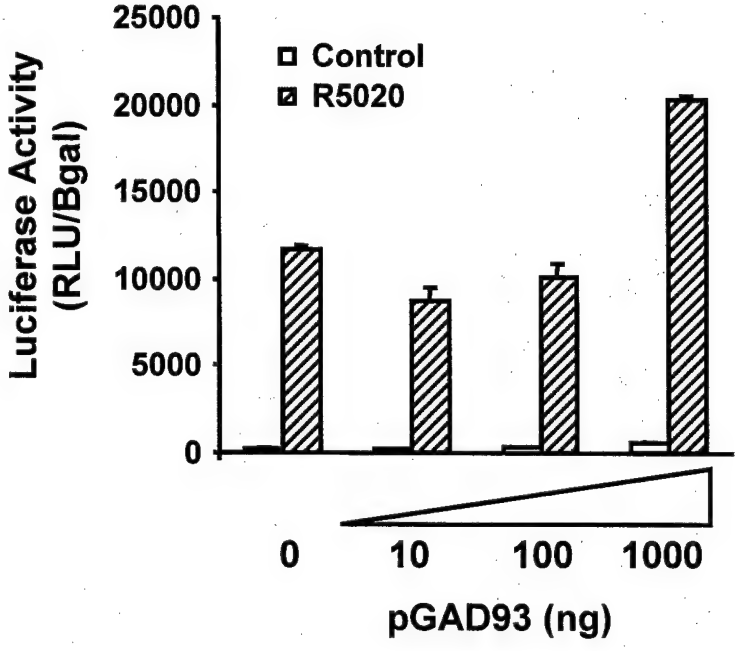
Luciferase Activity
(RLU/Bgal)
25000
20000
15000
10000
5000
0
Control
R5020
0
10
100
1000
pGAD93 (ng)

Fig.4.

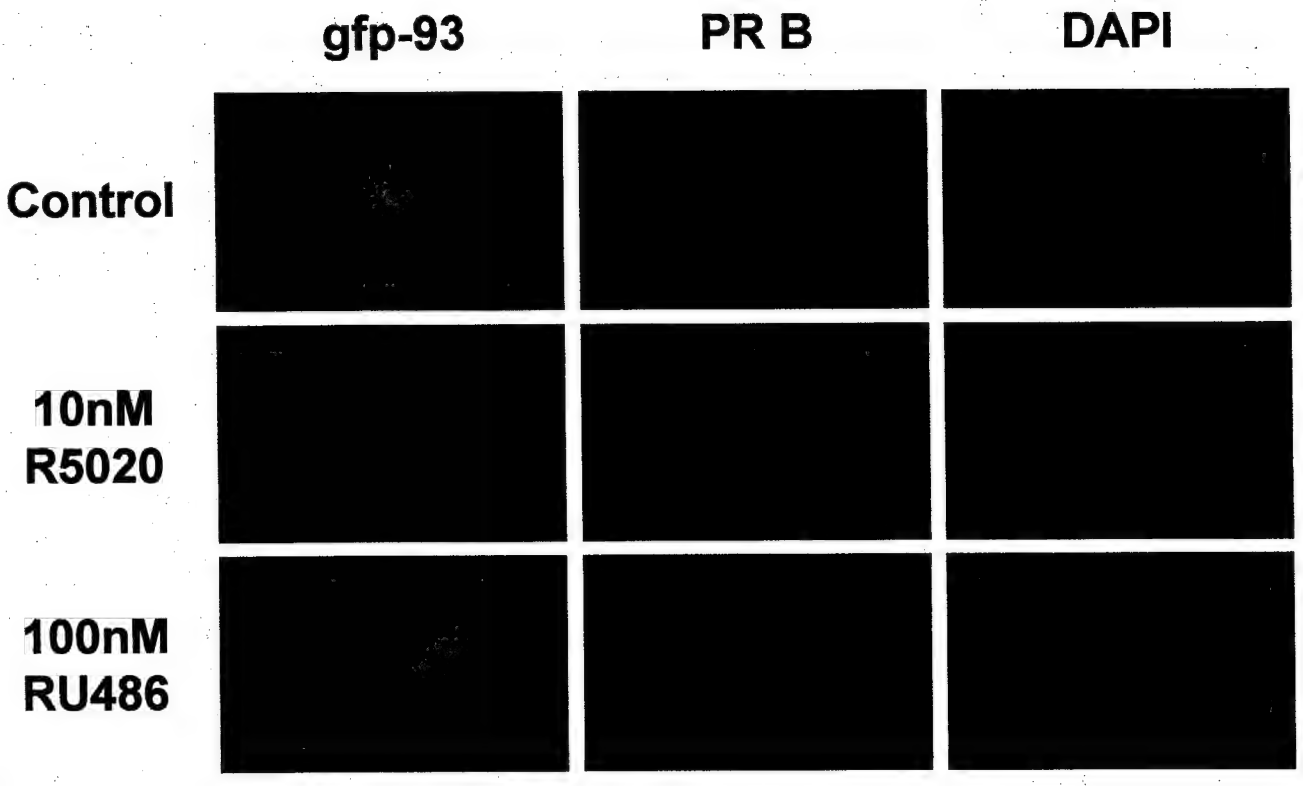

Fig.5

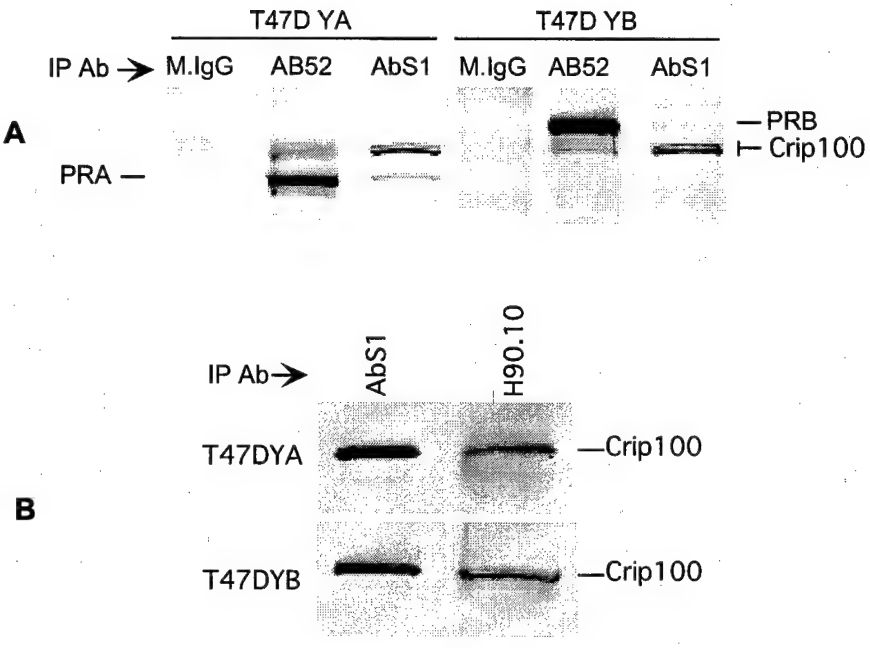
T47D YA
T47D YB
IP Ab
M.IgG
AB52
AbS1
M.IgG
AB52
AbS1
A
PRA
PRB
Crip100
IP Ab
AbS1
H90.10
B
T47DYA
Crip100
T47DYB
Crip100

Fig. 6

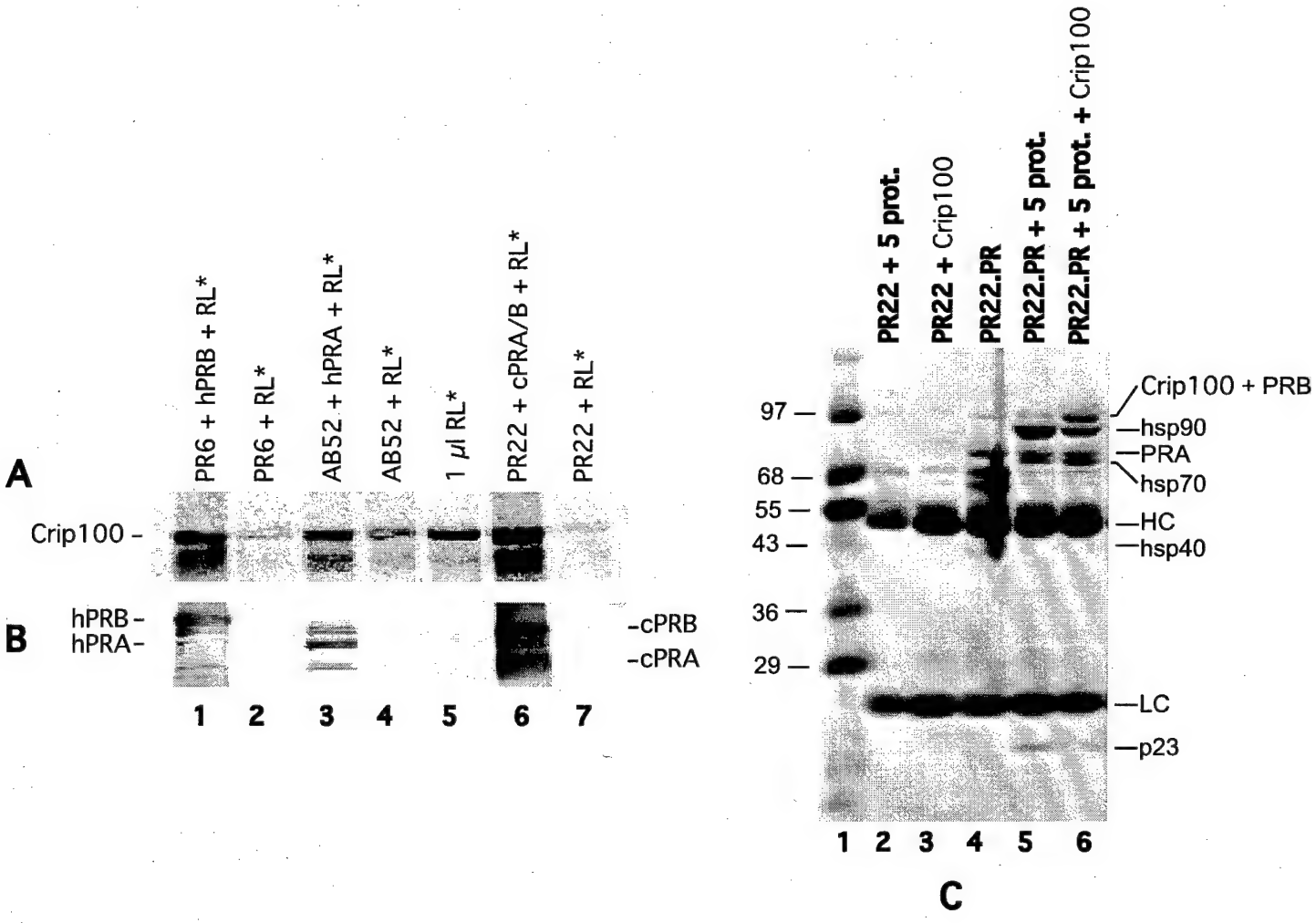
A
PR6 + hPRB + RL*
PR6 + RL*
AB52 + hPRA + RL*
AB52 + RL*
1 µl RL*
PR22 + cPRA/B + RL*
PR22 + RL*
Crip100 –
B
hPRB –
hPRA –
–cPRB
–cPRA
1 2 3 4 5 6 7
PR22 + 5 prot.
PR22 + Crip100
PR22.PR
PR22.PR + 5 prot.
PR22.PR + 5 prot. + Crip100
97 —
68 —
55 —
43 —
36 —
29 —
Crip100 + PRB
—hsp90
—PRA
hsp70
—HC
—hsp40
—LC
—p23
1 2 3 4 5 6
C

Fig. 7

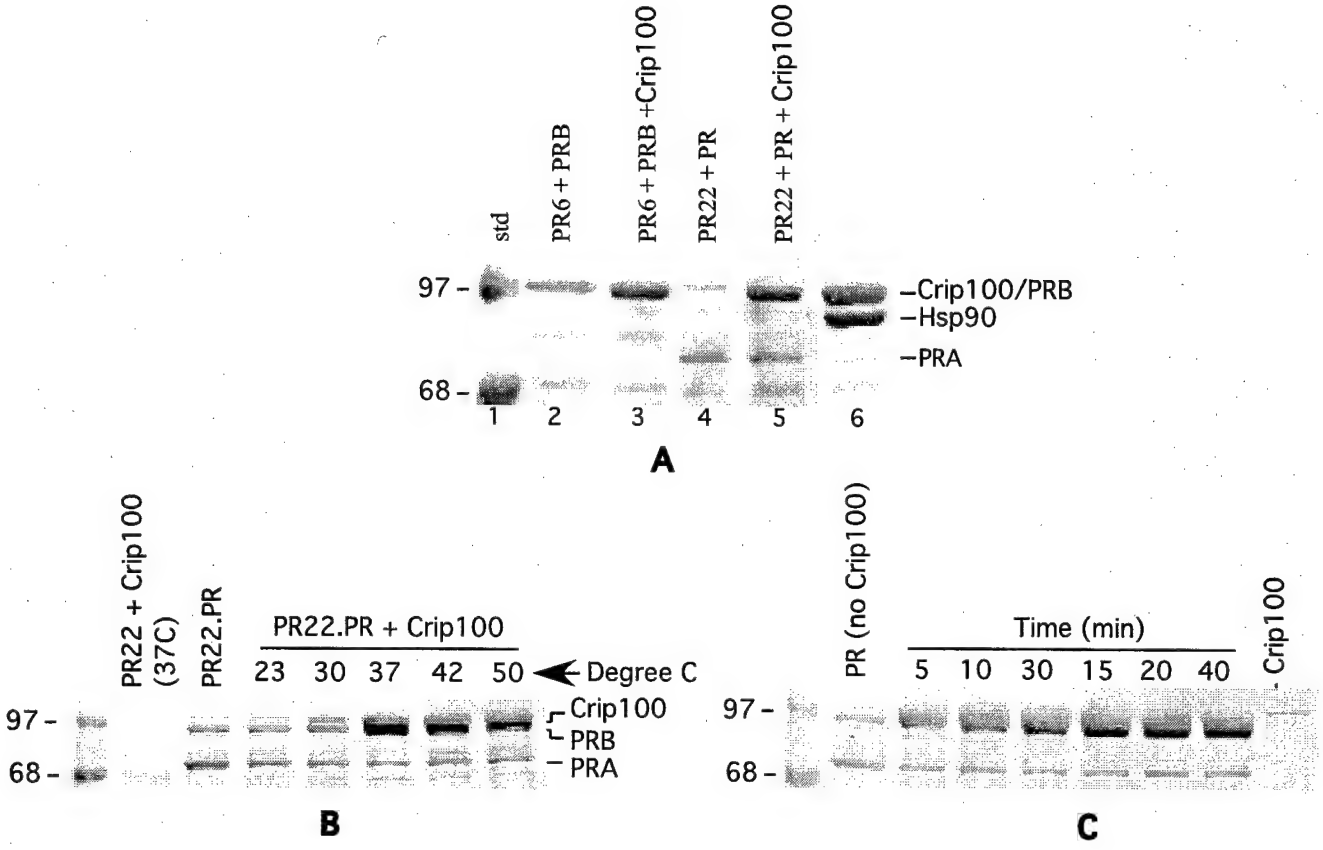
std
PR6 + PRB
PR6 + PRB +Crip100
PR22 + PR
PR22 + PR + Crip100
97 –
68 –
1 2 3 4 5 6
–Crip100/PRB
–Hsp90
–PRA
A
PR22 + Crip100 (37C)
PR22.PR
PR22.PR + Crip100
23 30 37 42 50
Degree C
Crip100
PRB
PRA
97 –
68 –
B
PR (no Crip100)
Time (min)
5 10 30 15 20 40
Crip100
97 –
68 –
C

Fig. 8

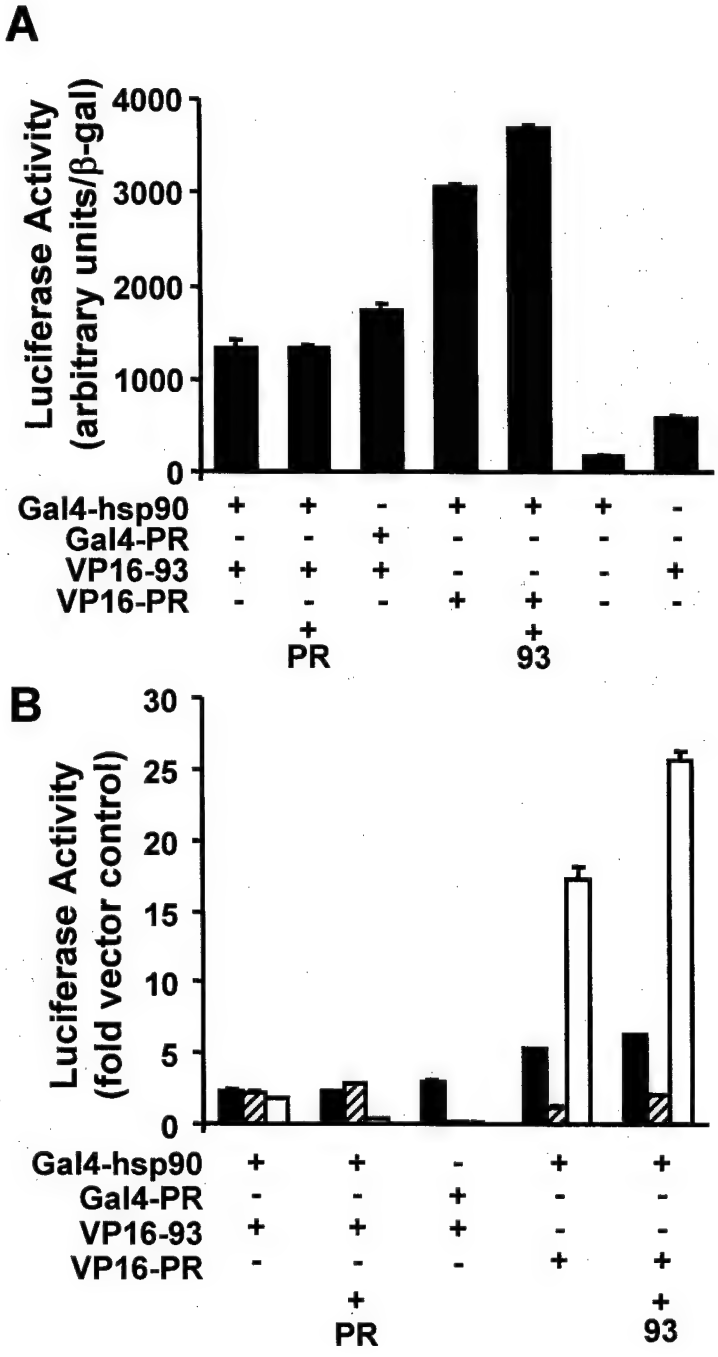
A
Luciferase Activity
(arbitrary units/β-gal)
4000
3000
2000
1000
0
Gal4-hsp90 + + - + + + -
Gal4-PR - - + - - - -
VP16-93 + + + - - - +
VP16-PR - - - + + - -
+
PR
+
93
B
Luciferase Activity
(fold vector control)
30
25
20
15
10
5
0
Gal4-hsp90 + + - + +
Gal4-PR - - + - -
VP16-93 + + + - -
VP16-PR - - - + +
+
PR
+
93

Fig. 9

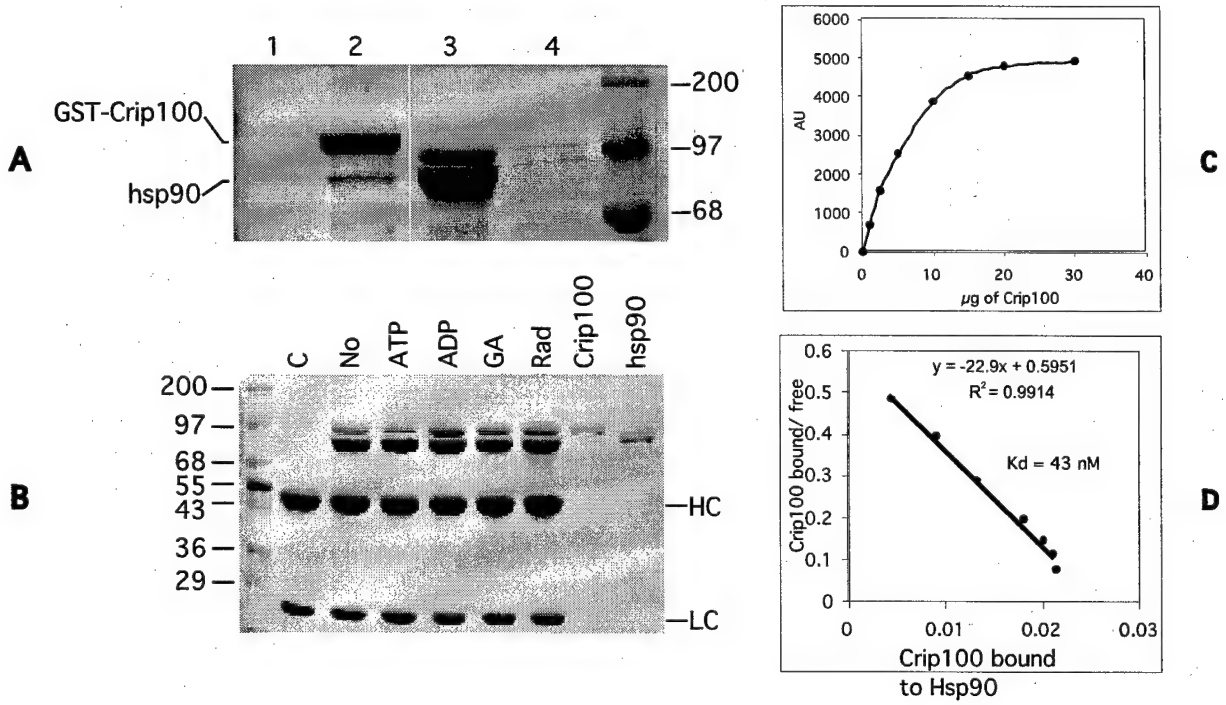
A
1
2
3
4
GST-Crip100
hsp90
200
97
68
B
C
No
ATP
ADP
GA
Rad
Crip100
hsp90
200
97
68
55
43
36
29
HC
LC
C
6000
5000
4000
3000
2000
1000
0
AU
0
10
20
30
40
μg of Crip100
D
y = -22.9x + 0.5951
R² = 0.9914
Kd = 43 nM
Crip100 bound/ free
0.6
0.5
0.4
0.3
0.2
0.1
0
0
0.01
0.02
0.03
Crip100 bound
to Hsp90

Fig. 10

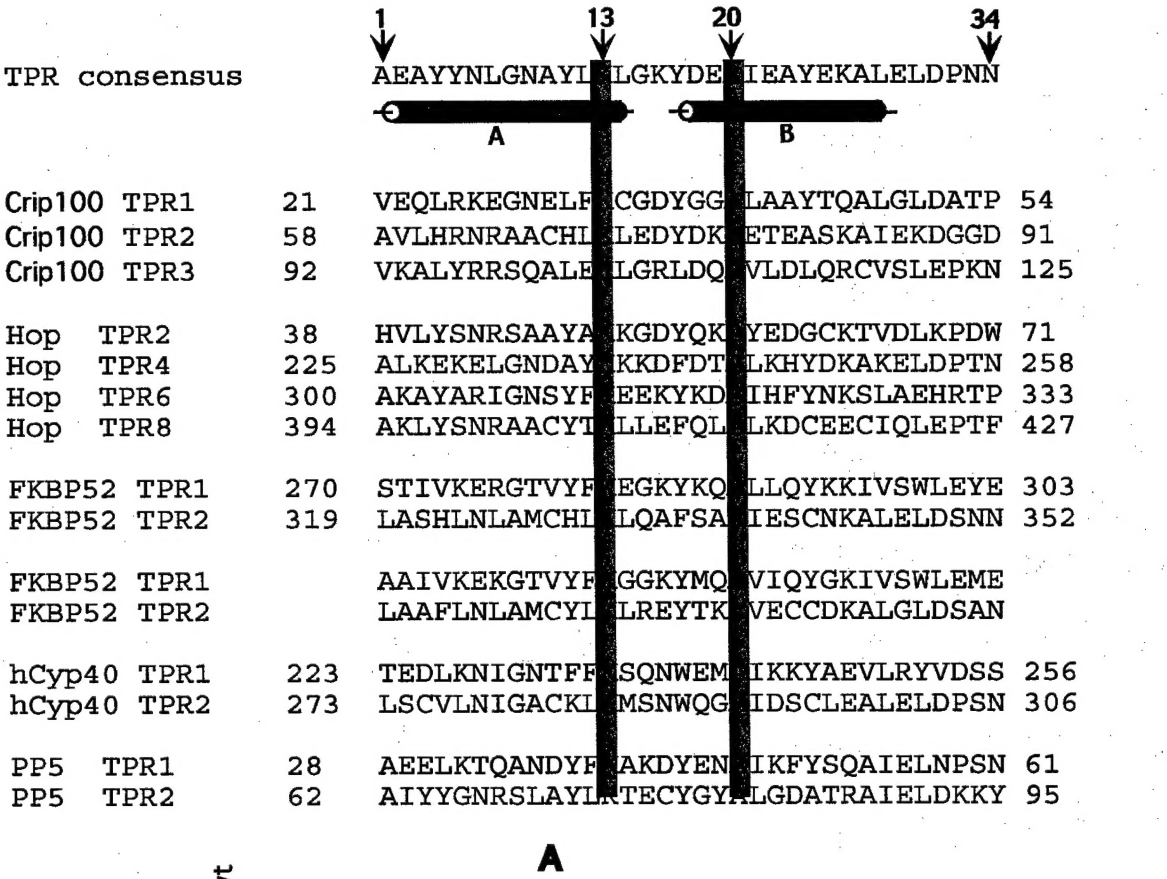
1
13
20
34
TPR consensus
AEAYYNLGNAYL LGKYDE IEAYEKALELDPNN
A
B
Crip100 TPR1 21 VEQLRKEGNELF CGDYGG LAAYTQALGLDATP 54
Crip100 TPR2 58 AVLHRNRAACHL LEDYDK ETEASKAIEKDGGD 91
Crip100 TPR3 92 VKALYRRSQALE LGRLDQ VLDLQRCVSLEPKN 125
Hop TPR2 38 HVLYSNRSAAYA KGDYQK YEDGCKTVDLKPDW 71
Hop TPR4 225 ALKEKELGNDAY KKDFDT LKHYDKAKELDPTN 258
Hop TPR6 300 AKAYARIGNSYF EEKYKD IHFYNKSLAEHRTP 333
Hop TPR8 394 AKLYSNRAACYT LLEFQL LKDCEECIQLEPTF 427
FKBP52 TPR1 270 STIVKERGTVYF EGKYKQ LLQYKKIVSWLEYE 303
FKBP52 TPR2 319 LASHLNLAMCHL LQAFSA IESCNKALELDSNN 352
FKBP52 TPR1 AAIVKEKGTVYF GGKYMQ VIQYGKIVSWLEME
FKBP52 TPR2 LAAFLNLAMCYL LREYTK VECCDKALGLDSAN
hCyp40 TPR1 223 TEDLKNIGNTFF SQNWEM IKKYAEVLRYVDSS 256
hCyp40 TPR2 273 LSCVLNIGACKL MSNWQG IDSCLEALELDPSN 306
PP5 TPR1 28 AEELKTQANDYF AKDYEN IKFYSQAIELNPSN 61
PP5 TPR2 62 AIYYGNRSLAYL TECYGY LGDATRAIELDKKY 95

A

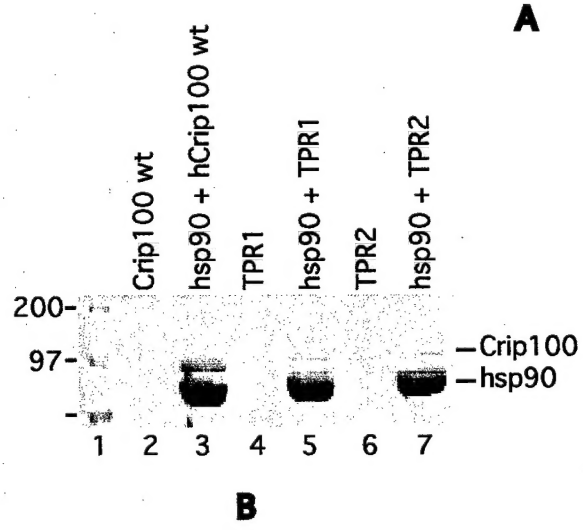
Crip100 wt
hsp90 + hCrip100 wt
TPR1
hsp90 + TPR1
TPR2
hsp90 + TPR2
200-
97-
-Crip100
-hsp90
1 2 3 4 5 6 7

B

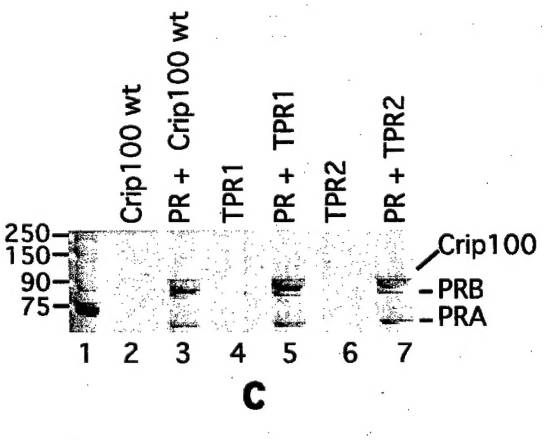
Crip100 wt
PR + Crip100 wt
TPR1
PR + TPR1
TPR2
PR + TPR2
250-
150-
90-
75-
Crip100
-PRB
-PRA
1 2 3 4 5 6 7

C

Fig. 11

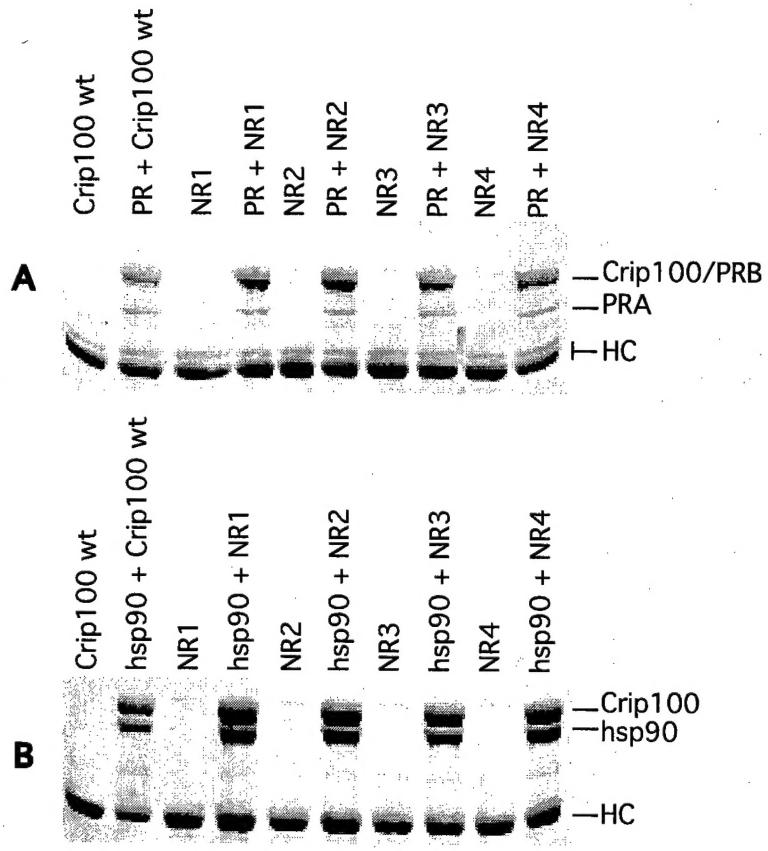

Target Construct	10-6 M RU486	Growth Assay	Color Assay
C-term wt	-	-	-
C-term wt	+	+	+
NRm 3	+	-	-
NRm4	+	+	+
none	-	-	-
none	+	-	-

C

Fig. 12

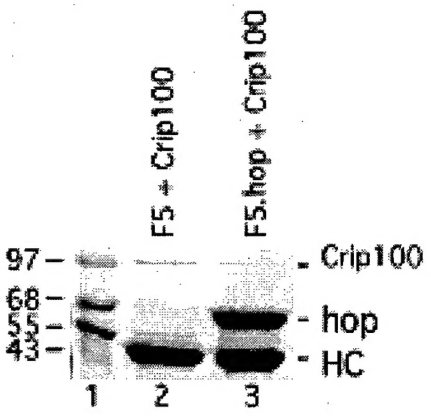
F5 + Crip100
F5.hop + Crip100
97
68
55
43
Crip100
hop
HC
1
2
3

A

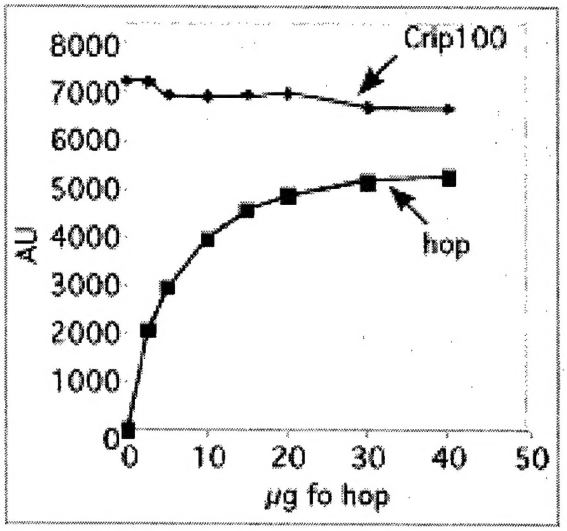
8000
7000
6000
5000
4000
3000
2000
1000
0
AU
Crip100
hop
0
10
20
30
40
50
µg fo hop

B

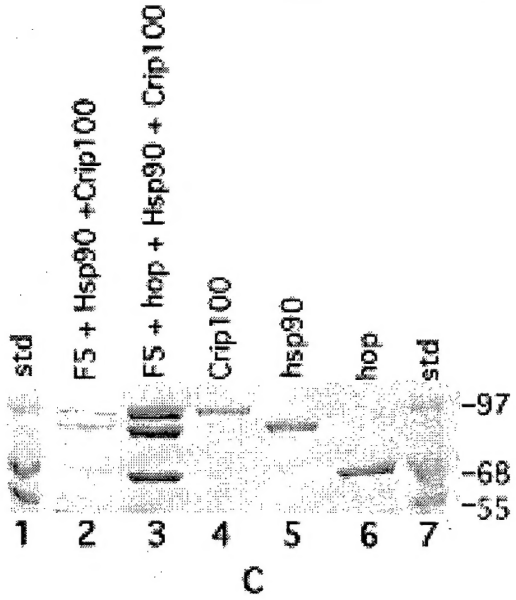
std
F5 + Hsp90 +Crip100
F5 + hop + Hsp90 + Crip100
Crip100
hsp90
hop
std
-97
-68
-55
1
2
3
4
5
6
7

C

Fig. 13

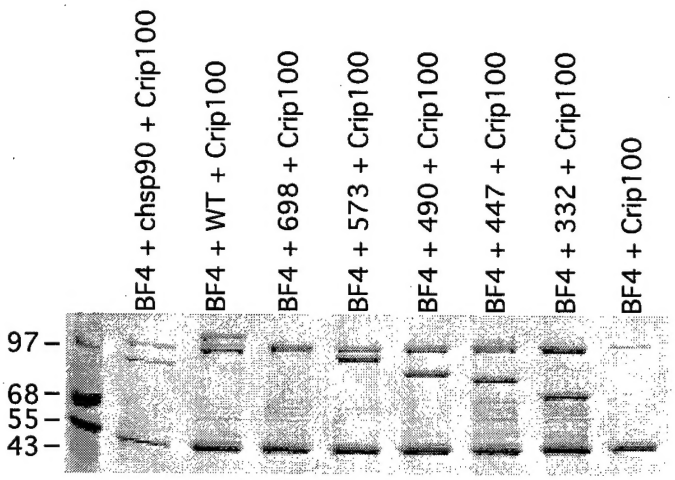
BF4 + chsp90 + Crip100
BF4 + WT + Crip100
BF4 + 698 + Crip100
BF4 + 573 + Crip100
BF4 + 490 + Crip100
BF4 + 447 + Crip100
BF4 + 332 + Crip100
BF4 + Crip100
97
68
55
43